DANMARKS OG GRØNLANDS GEOLOGISKE UNDERSØGELSE **RAPPORT 2025/31**

Processing of ultra-high resolution multi-channel seismic data offshore Denmark

Geological screening for offshore windfarms, the Danish Energy Agency

Sunny Singhroha, Rasmus Ørnekoll Stenshøj, Andreas Duus Petersen & Thomas Vangkilde-Pedersen

GEOLOGICAL SURVEY OF DENMARK AND GREENLAND
DANISH MINISTRY OF CLIMATE, ENERGY AND UTILITIES

G E U S

Processing of ultra-high resolution multi-channel seismic data offshore Denmark

Geological screening for offshore windfarms, the Danish Energy Agency

Sunny Singhroha, Rasmus Ørnekoll Stenshøj, Andreas Duus Petersen & Thomas Vangkilde-Pedersen

Thanks to Egon Nørmark, Sean Thomsen, Nicklas Christensen & Lis Allaart for their contribution to the work presented in this report.

GEOLOGICAL SURVEY OF DENMARK AND GREENLAND
DANISH MINISTRY OF CLIMATE, ENERGY AND UTILITIES

G E U S

Content

1. Seismic data acquisition overview

Ultra high-resolution seismic (UHRS) data were acquired by GEUS during geophysical surveys conducted in 2022 and 2023 on behalf of the Danish Energy Agency to support offshore wind farm development by improving subsurface geological understanding in key Danish offshore areas (Figure 1). The ENS 2022 survey, undertaken from November 14 to December 11, 2022, used the vessel Fortuna Crane to collect 3,291 km of UHRS data across six target areas (referred as Læsø North, LN; Læsø South, LS; Anholt South, AS; Vejsnæs Flak, VF; Køge-Krieger, KK and Bornholm, BO areas in this report; Figure 2) in the Kattegat, Inner Danish Waters, and the Baltic Sea (Pérez et al., 2023; Figure 2)). Despite weather-related interruptions, all planned survey legs were completed. The ENS 2023 survey, conducted between May 8 and June 2, 2023, employed the vessel Arctic Ocean for data acquisition in the Danish North Sea (Vangkilde-Pedersen et al., 2023; Figure 3). This campaign achieved 3,114 km of data acquisition out of a planned 4,400 km, again affected by weather delays. Seismic data from these two surveys provided enhanced coverage in areas with previously low seismic data coverage (Figure 1).

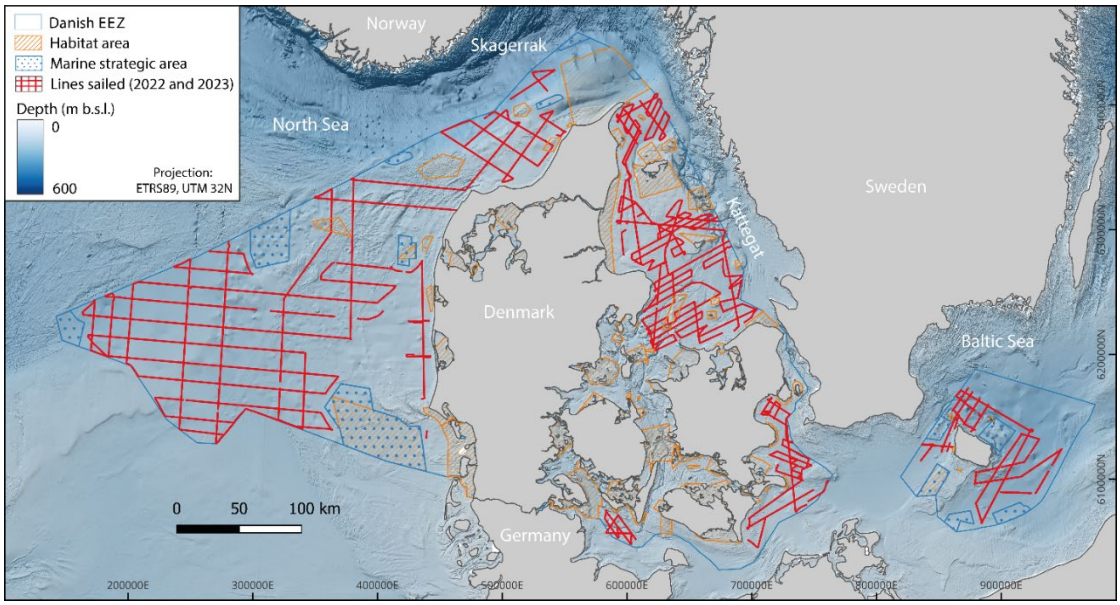

Figure 1 UHRS data acquisition (shown as red lines) during the ENS 2022 and ENS 2023 surveys.

Both the ENS 2022 and ENS 2023 surveys deployed a consistent suite of geophysical instrumentation, including single- and multi-channel sparker seismic systems, sub-bottom profiler, multibeam echo sounder, and side-scan sonar (Pérez et al., 2023; Vangkilde-Pedersen et al., 2023). For UHRS data acquisition, a Geo-spark 200 was used as the seismic source with a shot rate of 1.0 s and 0.5 s in the ENS 2022 and 2023 surveys, respectively. A Geo-spark 2000X / 1000 was used as the power supply and energy levels in the power supply were changed over the survey which resulted in changes in the source signature (Pérez et al., 2023; Vangkilde-Pedersen et al., 2023). The resulting source signature appears to have

100-1600 Hz and 100-1200 Hz bandwidths in the ENS 2022 and 2023 surveys, respectively. There appears to be a high amplitude notch noise around 380 Hz in most of the data from the ENS 2022 survey. The seismic sample rate was 0.0625 ms and 0.125 ms in the ENS 2022 and 2023 surveys, respectively.

Variations in the instrument availability and deployment configurations led to slight differences in the acquisition of the UHRS datasets between the two surveys. One of the most significant differences involved changes in the source-receiver geometry, as well as in the number of seismic channels and GPS positioning systems used. In the ENS 2022 survey, the UHRS system comprised 96 channels with 1-meter spacing, deployed approximately 5 to 9 meters (distance kept changing due to changes in intensity and direction of ocean waves, ship sail direction and overall weather condition) portside from the source. GPS positioning was available at two locations—on the source and on the ship. The first and last eight channels of the streamer array were composed of oil-filled digital streamers, while the remaining channels comprised GeoEel Solid LH-16 sections with 1-meter channel spacing. It was also observed that the streamers were towed 3–6 meters further aft relative to the source. As a result of this configuration, the nearest high-quality GeoEel Solid LH-16 channel was typically positioned 12–18 meters from the sparker source.

In contrast, the ENS 2023 survey utilized 48 channels with 1-meter spacing, similarly placed 3 to 9 meters portside from the source. However, in this configuration, the start of the streamer was positioned approximately 8 meters closer to the ship relative to the source. Similar to 2022, the first and last eight channels comprised oil-filled streamers, while the remaining channels were GeoEel Solid LH-16 sections. This geometry resulted in the nearest GeoEel Solid LH-16 channel being positioned only 3–9 meters from the sparker source, thereby improving near-offset coverage. Additionally, in this survey, GPS receivers were installed at four positions: on the source, on the ship, and at both the start and end of the streamer, providing more accurate spatial positioning and geometry control. These differences in acquisition geometry and number of recorded GPS locations contributed to variations in data quality and influenced the subsequent seismic data processing strategies.

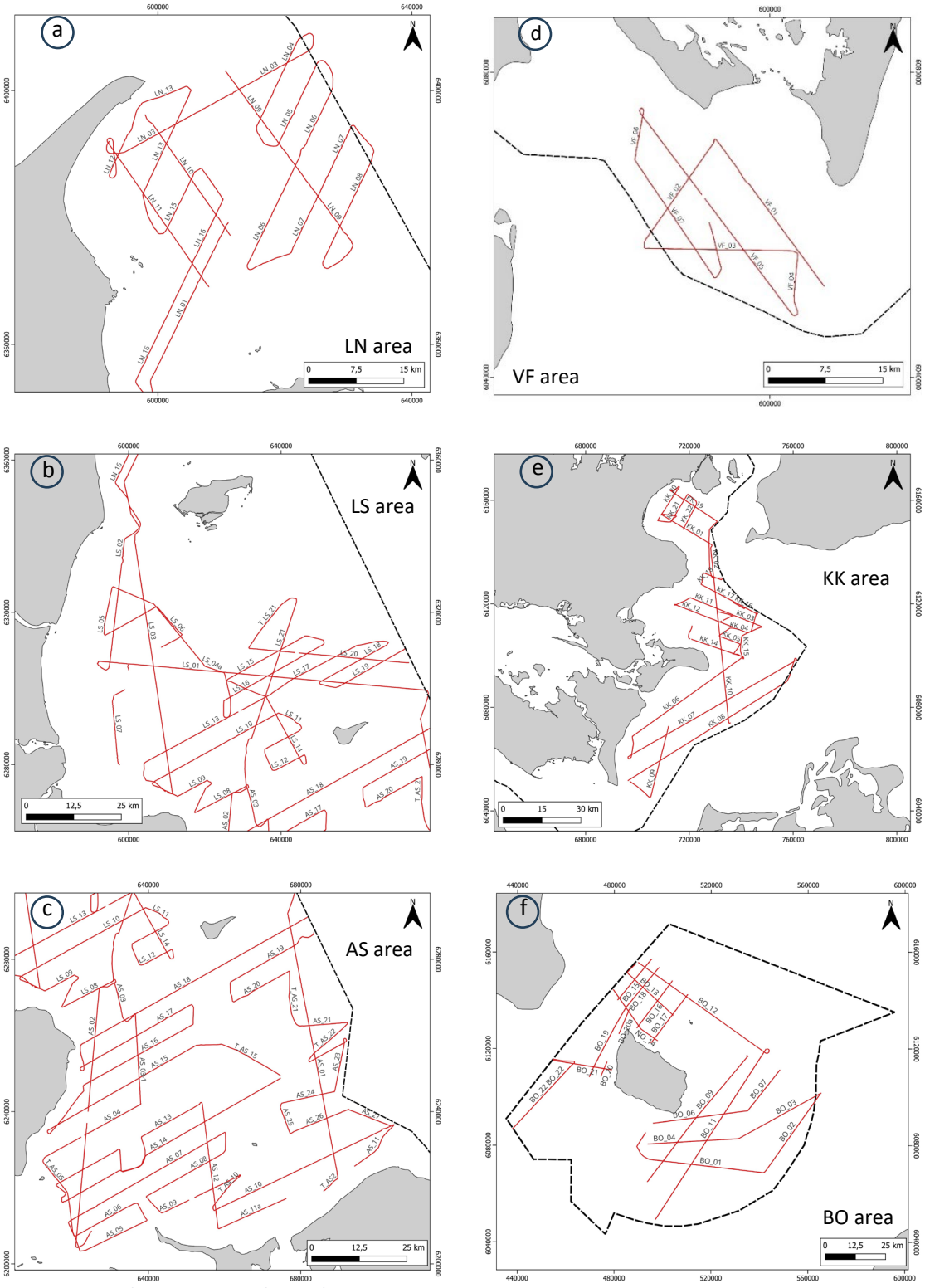

Figure 2 UHRS data acquisition during the ENS 2022 survey.

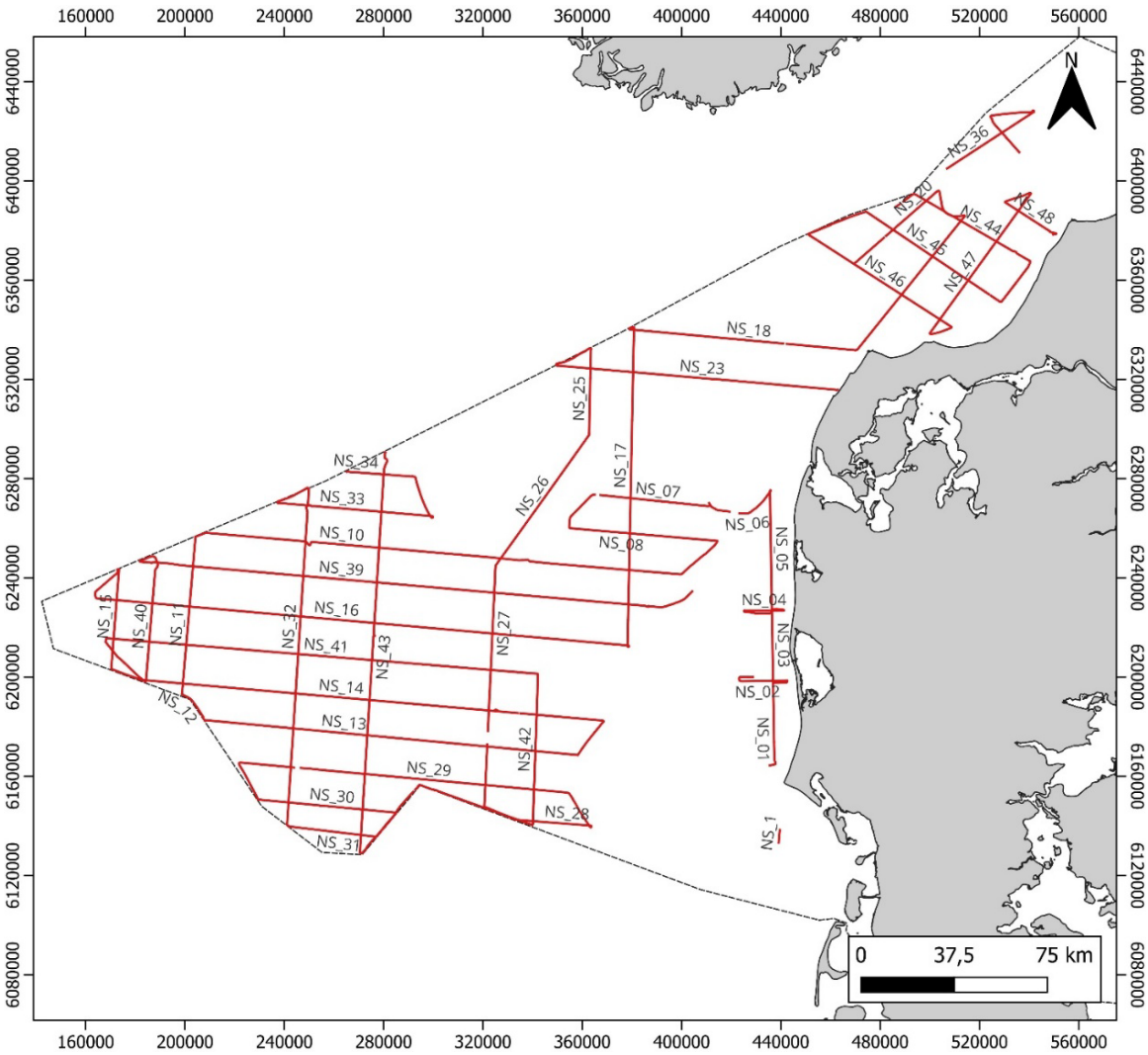

Figure 3 UHRS data acquisition during the ENS 2023 survey.

2. UHRS data processing workflow

Multi-channel seismic data processing was performed in RadExPro, which provides specialized modules for UHRS processing. The standard workflow included: geometry assignment, data quality control (QC) and binning, filtering and noise suppression (bandpass filtering, f-k filtering, burst noise removal, TFD noise attenuation, etc.), multiple removal, swell correction, deghosting, deconvolution, stacking, migration, and necessary amplitude corrections. However, the workflow was not applied uniformly; adjustments were made according to data quality, acquisition geometry, and geological variability within and between surveys.

Key factors influencing processing adjustments
Several (mostly acquisition related) parameters necessitated modifications to the processing strategy, including:

- Variation in the number of streamers used across survey legs;
- Differences in source–streamer geometry, influencing available offset ranges;
- Variability in number of recorded locations using GPS;
- Weather conditions, affecting noise levels and swell-induced static issues;
- Changes in water depth creating variability in multiples and incidence angles;
- Source signature variability, altering signal bandwidth and amplitude;
- Seafloor character, influencing deconvolution and strength of multiples; and
- Computational capacity, which changed over time and impacted processing routine.

Each factor required targeted adjustments to ensure optimally processed seismic data with optimal imaging resolution, signal fidelity, and interpretability across all survey regions. Despite varying acquisition conditions, the core processing philosophy remained consistent between the North Sea and Inner Danish Waters datasets. The ENS2023 survey data from the North Sea benefited from better source-receiver geometry and complete GPS positioning, enabling a more standardized workflow. Conversely, data from the ENS 2022 survey, characterized by typically shallower water depths, variable seafloor reflection strengths, and GPS coverage of only the seismic source, required enhanced geometry reconstruction, customized amplitude corrections, and additional filtering.

In this report, line numbers are interchangeably used in two formats (for example, for line 17 in the North Sea, it is referred to as NS_17 and also as Line17_NS).

Single-channel seismic data was processed on-board using GeoSuite software, with additional processing carried out in RadExPro for selected datasets (Vangkilde-Pedersen et al., 2025). Details of the on-board single-channel seismic data processing are available in Vangkilde-Pedersen et al. (2025). A short summary is given below.

The seismic data was first georeferenced by assigning each trace a geographic location using shipboard GPS data and the known offset between the GPS antenna and the streamer, with an estimated positional uncertainty of about 10 meters. A bandpass filter (50–2500 Hz)

was applied to enhance the signal quality and suppress noise. Swell-induced static issues were corrected by applying a static shift based on sea conditions, with different trace window lengths for long- and short-period swells. Data above the seafloor reflection was muted to eliminate unwanted water column noise. Trace mixing was applied to smooth lateral variations, and spiking deconvolution was used to improve vertical resolution by extracting a zero-phase wavelet from a representative trace. Time-variant gain correction was applied to compensate for spherical divergence, and Automatic Gain Control (AGC) was used in areas with weaker signal quality. For datasets from shallow water areas in the inner Danish waters, additional processing steps in RadExPro included noise attenuation, burst noise removal, deghosting, and migration.

3. Geometry assignment and positioning issues

Geometry assignment represents the first and most fundamental step in seismic data processing. It involves accurately assigning spatial coordinates to each seismic trace by defining the precise locations of both the seismic sources and receivers. Correct geometry is essential, as any spatial inaccuracy directly affects subsequent processing steps and the final subsurface image. In the ENS 2023 survey, we achieved high positional accuracy through the use of four GPS units strategically positioned: one mounted on the ship, one at the seismic source, and two at the front and tail of the streamer. This configuration provided robust spatial referencing for both the source and the receiver array throughout most of the survey. However, during acquisition, portions of the GPS data were compromised by repetitive readings, resulting in missing positional information (Figure 4). The duration of these data gaps varied significantly, ranging from less than a second to several minutes and sometimes even hours. To correct these gaps, we employed linear interpolation between the nearest valid GPS data points, ensuring continuous spatial coverage.

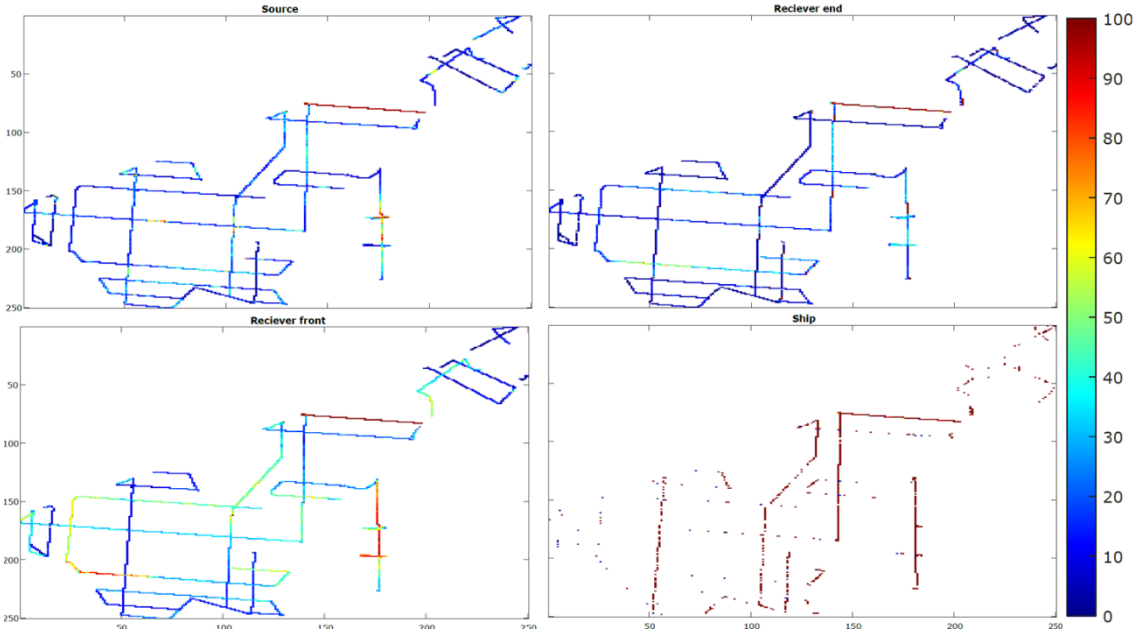

Figure 4 Distribution of missing (in %) GPS records in ship, source, start and end of the streamer in the ENS 2023 survey.

Once the missing GPS intervals were corrected, the receiver positions were calculated using the coordinates of the GPS units at the front and tail of the streamer. Since there was a small but measurable distance between the GPS antennas and the first and last receivers (the 1st and 48th channels), these offsets were explicitly accounted for when computing the receiver locations. This careful treatment of geometry, including the correction of missing GPS data, interpolation, and consideration of physical offsets, ensured a high degree of positional accuracy, estimated to be within approximately one meter. Such precision provides a reliable foundation for subsequent processing stages, including velocity analysis, stacking, and migration. The assigned geometry was quality checked by creating plots to understand the variations in distances between different GPSs (Figure 5). In North Sea, for two lines (Line

47 and 48), navigation files did not record any data, hence creating high uncertainty in the assigned locations as the traces have been assigned locations by simply interpolating the beginning and end of the lines available in the survey log. Position accuracy is expected to be within 1 m in areas where GPS data is recorded consistently (blue areas in Figure 4) and the CDP position accuracy to a few (1-10) meters in areas where data recording is relatively inconsistent depending on how long the breaks in the recording are (red areas in Figure 4). The plots in Figure 5 were created for each line and potential issues were identified as such issues created anomalous values in the plot.

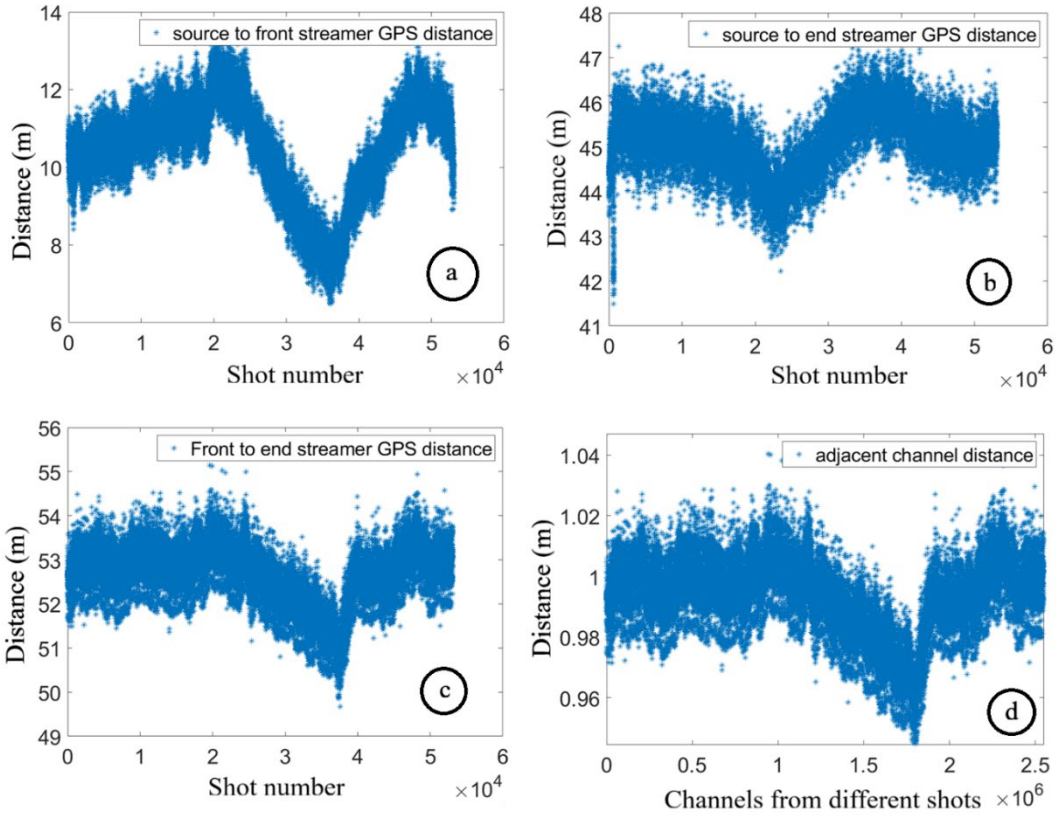

Figure 5 Distance between the source and the front GPS (a), between the source and the tail GPS (b), between the front and end-of-streamer GPS (c), and between adjacent channels (d) in the assigned geometry for Line 26 in the North Sea.

In contrast, the ENS 2022 survey dataset was recorded with only two operational GPS units, located on the ship and at the source. The absence of dedicated GPS units along the streamer introduced increased uncertainty in the receiver positions. To better constrain the geometry, we analyzed direct arrival times and their variation with increasing offset, applying travel-time-based corrections to more accurately estimate receiver locations and reduce spatial uncertainty (Figure 6). However, this analysis has been done only over few shots for each line. Changes in source receiver geometry within the line are not corrected for in the processing.

Furthermore, in the ENS 2022 survey, the GPS data also occasionally exhibited temporal gaps, ranging from a few seconds to several minutes, depending on the survey line. In instances where the GPS signal was intermittent or unreliable, we applied interpolation techniques to fill the missing data, thereby preserving spatial continuity and ensuring consistent geometry throughout the dataset. However, in cases where significant gaps in the recorded locations were present, ship locations were used for assigning source locations and locations of receivers as well. This created relatively high uncertainty in the receiver locations. However, it is expected that the relative geometry will remain the same thereby creating offset accuracy to same level. Processing is more sensitive to offset values. Any inaccuracy in the position of source and receiver can potentially create erroneous binning of traces but if offsets are similarly affected (within 5-10% either positively or negatively), the effect on the processing is minimal.

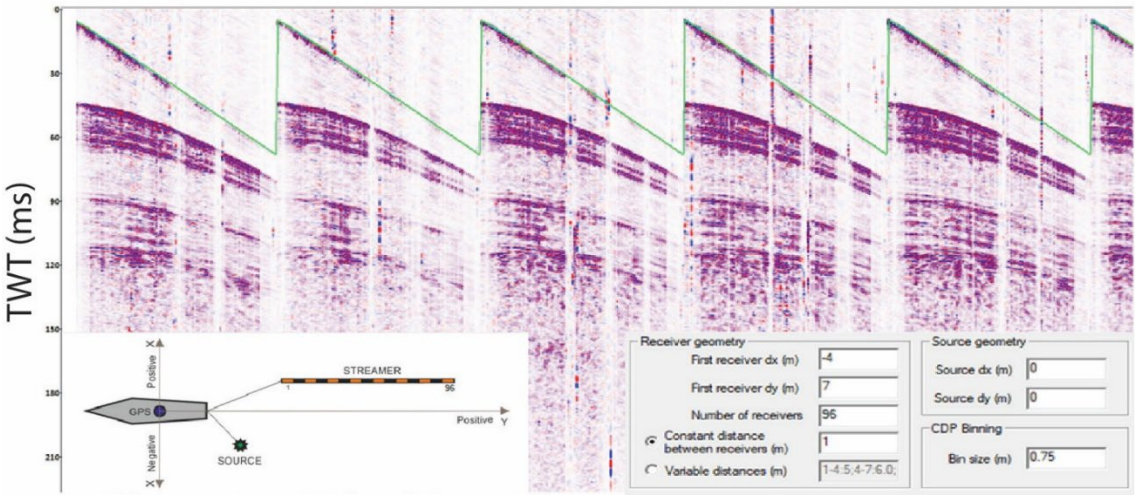

Figure 6 Shot gathers for shot numbers 584000-584005 and estimated direct arrival time (shown in green color) based on offset estimates (from the source-receiver geometry) and using 1.48 km/s water velocity.

4. Data QC and binning

A detailed data quality assessment was carried out to evaluate the performance of each channel in the acquired data. In the ENS 2023 survey, channels from the oil-filled streamers generally exhibited lower performance compared to those from the GeoEel Solid LH-16 digital streamers. Also, the polarity of data from oil filled streamers was opposite to the data from GeoEel Solid LH-16 streamers which needed correction to make data polarity uniform for all the acquired channels. Among the 32 channels in the GeoEel Solid LH-16 sections, channels 9–23 and 29–36 demonstrated slightly better performance than channels 24–28 and 37–40. However, these variations were not consistent across all acquisition lines. Despite the differences, all channels contributed positively to enhancing the seismic signal quality and reducing noise in the stacked sections. On very few lines affected by swell noise, where seafloor picking in the pre-stack domain was important, only channels 9-23 and 29-36 were used for further processing (details discussed later in section 6).

To ensure accurate Common Depth Point (CDP) assignment, a crooked-line geometry workflow was implemented. CDP binning was performed after calculating the midpoints between sources and receivers, followed by binning the traces into 0.75–1.0 m bins. Traces with a source-receiver mid-point offset more than 3.5-7.0 m perpendicular to the sail direction were excluded from the dataset to minimize the relative effect of sideswipes or potential location related issues (erroneous GPS reading can create erroneous location of traces affecting offset estimates). On very few lines affected by swell noise, where manual seafloor picking in the pre-stack domain was important, CDP bin size was kept at 1.25 m, to ensure that the CDP fold was consistent with other processed datasets.

In the ENS 2022 survey, a similar trend was observed: channels from oil-filled streamers performed poorer than those from the GeoEel Solid LH-16 streamers. Due to the shallower water depths compared to the North Sea, data quality from far offset was notably affected by amplitude variations with offset (AVO) effects, which resulted in strong shallow reflections and limited energy penetration at deeper depths for far offsets. In addition, multiple reflections were considerably stronger than the primary signals. NMO stretch effects were also more pronounced at these shallow depths, necessitating muting to preserve data quality. In areas with limited penetration, inclusion of far-offset data provided minimal improvement to the final stacked image. Channel filtering was therefore performed based on both individual channel performance and its contribution to the quality of the stacked section. Only channels that demonstrably improved the signal-to-noise ratio were retained, extending the offsets up to the point where further inclusion no longer enhanced the stacked image.

For the ENS 2022 survey geometry, the Marine Geometry Input module in RadExPro was used for CDP binning. In this workflow, Geometry was assigned using the relative positioning of receivers from the source which is recorded by the GPS. Data without any assigned CDPs were subsequently filtered out to ensure data consistency and reliability.

5. Filtering

Filtering enhances signal quality by attenuating unwanted frequency components and coherent or incoherent noise. The primary filtering methods applied include:

Bandpass Filtering: The exact filter parameters were adjusted depending on the noise characteristics of each line, however, a bandpass filter of 50–100–1600–2000 Hz was applied to most lines at the beginning of the processing. North Sea data generally contained useful signal frequencies up to ~1200 Hz (Figure 7; Figure 8), while inner Danish waters showed signal energy up to 1500 Hz.

Notch Frequency Removal: We observed narrow-band noise, particularly between 380–400 Hz, in the ENS 2022 survey data. This was addressed using a notch filter.

F-K (Frequency–Wavenumber) Filtering: This method was applied to NMO-corrected shot gathers to remove coherent linear noise by distinguishing signals based on their apparent dip in the frequency-wavenumber domain (Figure 7; Figure 8). The selection of F-K polygon was made considering the noise level.

Burst Noise Removal: High-amplitude, short-duration noise spikes were identified and suppressed using burst detection algorithms that replaced the affected samples with interpolated or smoothed values (Figure 7; Figure 8). The selection of parameters was made considering geological conditions in an area and considering the data quality. Parameters used for Line07_NS (Figure 7) in RadexPro module for Burst noise removal are:

- Window size for average value calculation: 11 traces
- Rejection percentage: 75%
- Do not change amplitude lower than (%) of the amplitude: 25%
- Modify values when exceed average in more than N times: 4

TFD (Time-Frequency Domain) Noise Attenuation: Time-Frequency Domain (TFD) Noise Attenuation in RadExPro is crucial for removing non-stationary, time-varying noise without distorting the seismic signal. It enhances weak reflections and improves overall data clarity, especially in complex or noisy environments. Parameters used for Line07_NS (Figure 7) in RadexPro module for TFD Noise Attenuation are:

- Time window width: 5 ms
- Tapering: 15%
- Processing frequency interval: 100-1500 Hz
- Aperture: 4 traces
- Threshold: 1.5

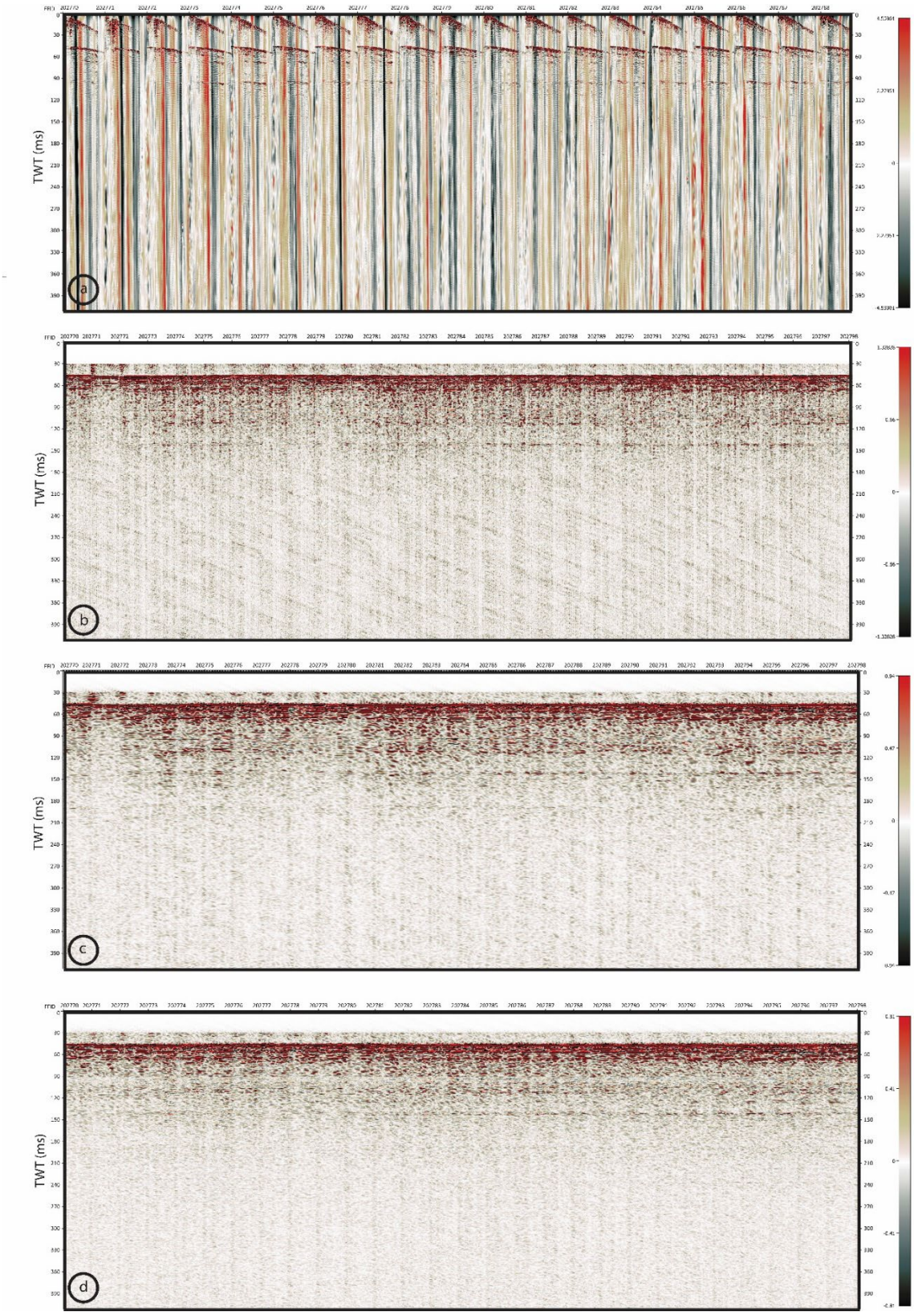

Figure 7 Shot gathers for Line07_NS: (a) raw data, (b) after data filtering, bandpass filtering, NMO correction and pre-stack demultiple, (c) after FK filtering, and (d) after burst and TFD noise removal.

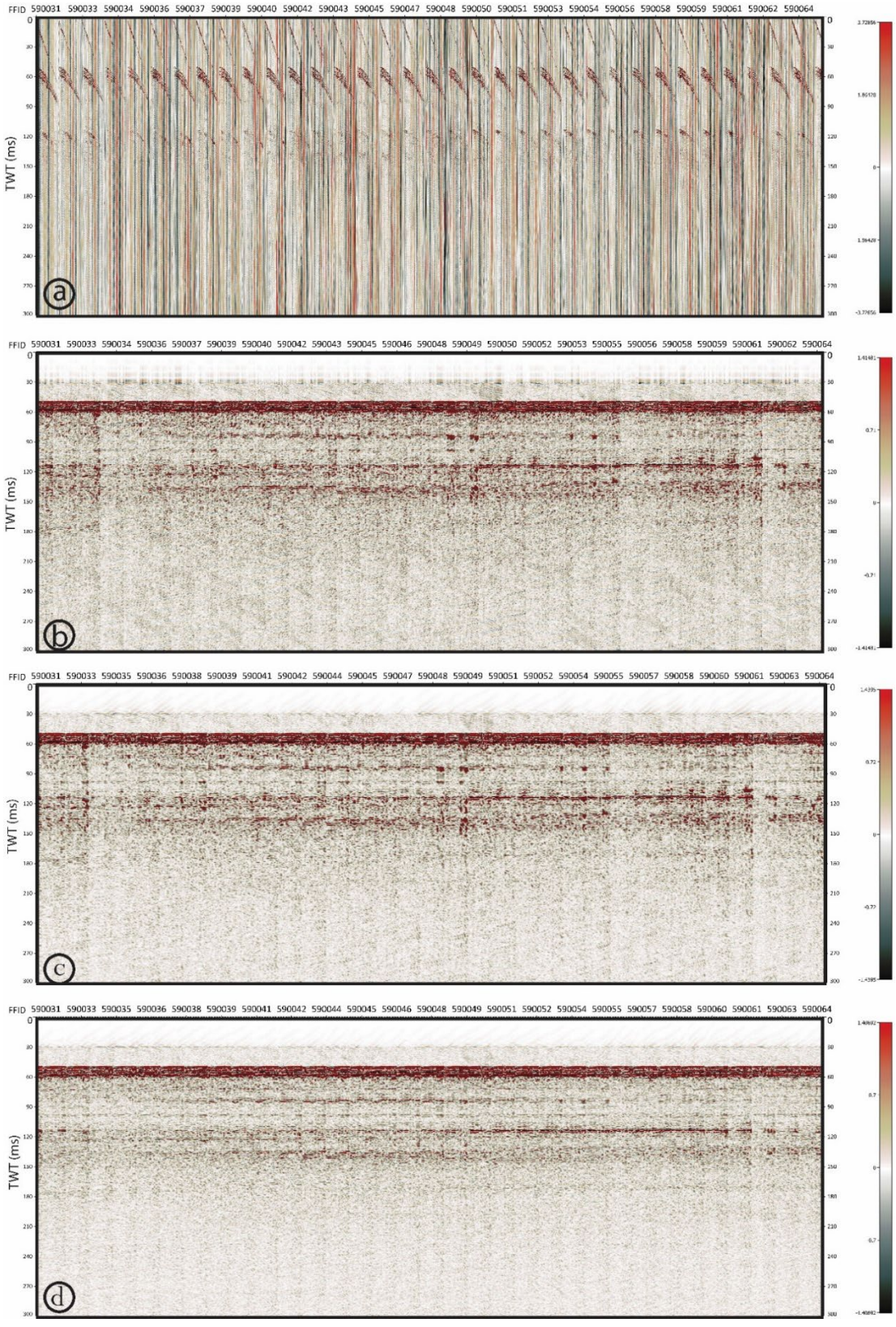

Figure 8 Shot gathers for Line19_AS: (a) raw data, (b) after data filtering, bandpass filtering, NMO correction and pre-stack demultiple, (c) after FK filtering, and (d) after burst and TFD noise removal.

6. Swell induced static issues

Swell-induced motion of seismic equipment is particularly problematic in ultra-high-resolution seismic (UHRS) data due to its short wavelength (~1–1.5 m). In such cases, static variations caused by swells can become comparable to the seismic wavelength, leading to destructive interference during stacking. To manage this, the acquired data were categorized based on the severity of observed swell effects (Figure 9):

- No swell: within ¼ of the seismic wavelength
- Little swell: within ½ of the wavelength
- Swell: between ½ and one wavelength
- Severe swell: greater than one wavelength

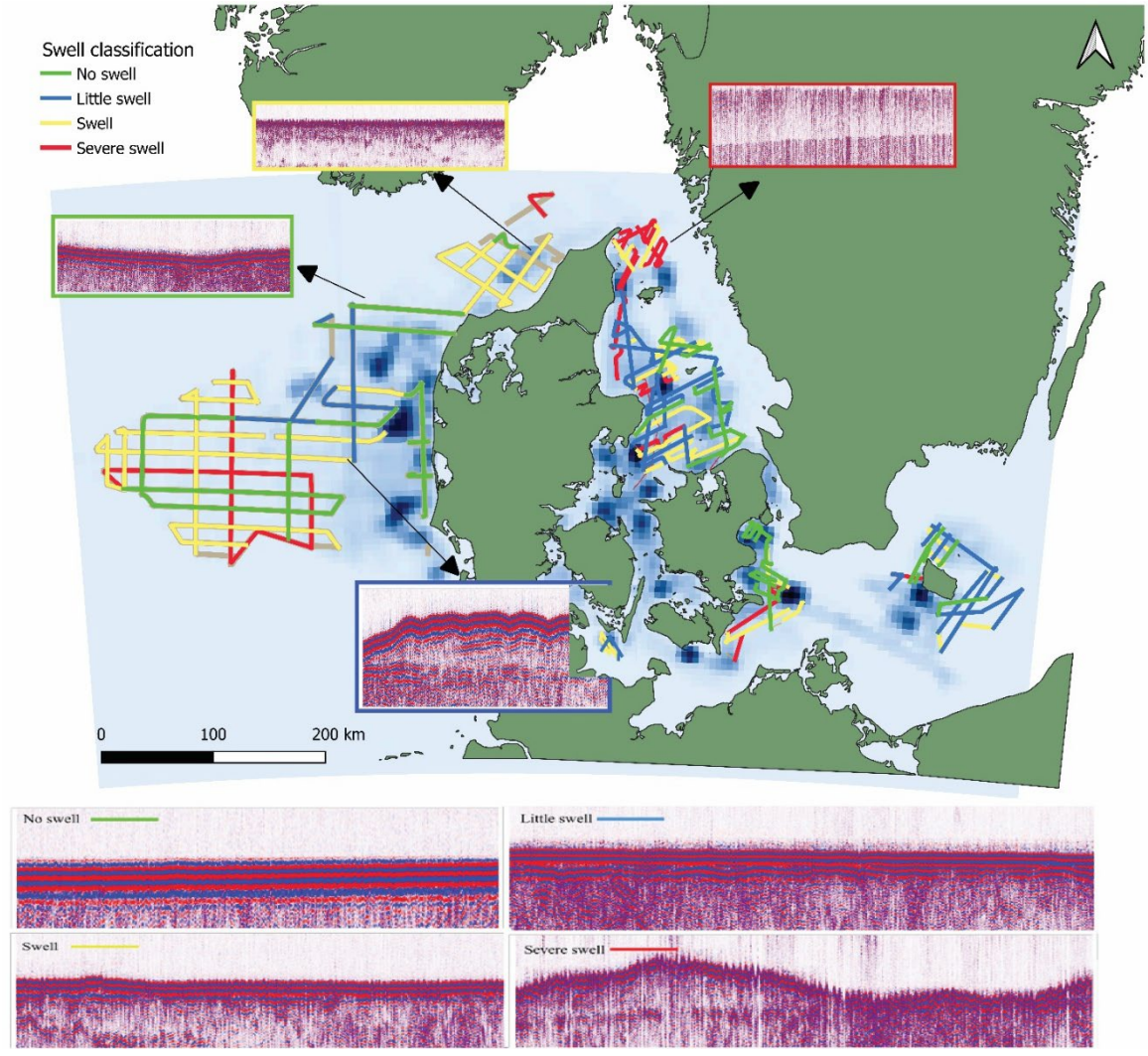

Figure 9 Classification of acquired data in swell categories.

Although somewhat subjective, this classification provided a practical framework for determining the appropriate processing workflow. To correct for swell effects, seafloor reflections

were picked on pre-stack data. For lines showing minimal swell (less than ¼ wavelength), no correction was applied (Figure 9; Figure 10). Similarly, swell correction was omitted for areas of lower strategic importance due to the labor-intensive nature of manual picking. Based on these criteria, 26 lines from the ENS 2023 survey were corrected for swell effects: Lines 01, 07, 10, 14–17, 19–21, 30–34, and 39–48_NS (Figure 11 shows the effect of swell correction on Line07_NS).

Accurate seafloor picking in pre-stack seismic data is essential for reliable swell correction. Two picking methods were used:

- Semi-automated approach: applied to Lines 01, 07, 10, 17, 33, 34, and 45–48.
- Manual approach: applied to the remaining lines, which were considered of higher strategic importance.

Manual seafloor picking achieved nearly 100% accuracy, producing very high-quality results. For most manually picked lines, channels 9–23 and 29–36 were used, while the semi-automated approach utilized channels 9–39 and occasionally also channel 40. In some cases, the semi-automated method was first used to generate preliminary picks, which were then refined manually.

Semi-automated approach for seafloor picking in Pre-stack data

RadExPro offers multiple methods for seafloor picking. Among them, threshold-based picking proved most effective. In this approach, a pick is made when the amplitude exceeds a specified threshold value. However, the optimal threshold varied across channels and FFID ranges, likely due to changes in seafloor reflectivity, AVO (amplitude variation with offset) effects, water depth and gradual changes in sparker energy output over time. Determining these optimal thresholds manually for each range was nearly as time-consuming as full manual picking. To streamline this process the following workflow was adopted, here referred to as the semi-automated approach:

- Preprocessing: After applying deghosting, top muting (to remove direct arrivals) and bandpass filtering, the peak amplitude value for each trace was exported.
- Amplitude Profiling: Peak amplitudes were imported into a MATLAB script to generate a peak amplitude profile. This profile guided the selection of FFID ranges for threshold tuning in RadExPro.
- Threshold Interpretation: Optimal threshold values were interpreted in RadExPro for a small subset of data to understand the relationship between peak and optimum threshold amplitudes.
- Segmentation of the seismic line in FFID ranges: The number of distinct threshold intervals was decided based on the amplitude variability.
- Scaling and Output: Once the interpreted thresholds were satisfactory, the “output” option was enabled to generate a header file containing FFID, CHAN, and scaling ratios to normalize traces to the highest threshold. The displayed threshold value from the MATLAB code was then used in RadExPro to ensure uniform scaling across all intervals and channels.

- Quality Control: The generated header was imported, and QC was performed to verify consistent picking quality across channels. Diagnostic plots from the MATLAB script were used to identify any anomalous channel behavior.

During seafloor picking, the applied threshold values were intentionally kept on the higher side to minimize the occurrence of mispicks (Table 1). Mispicks, in this context, refer to instances where an incorrect seafloor reflection is picked, for example, when the seafloor pick alternates between the first and second positive amplitude phases, or when it erroneously picks a reflection occurring a few milliseconds below the true seafloor. Mispicks are particularly problematic because they lead to incorrect static corrections, which in turn amplify noise in the stacked seismic section. By maintaining relatively high threshold levels, the workflow prioritized accuracy over completeness—resulting in a larger number of missing picks (traces where the threshold was never reached) rather than incorrect ones (Figure 10a–c).While this approach effectively reduced mispicks, it introduced a secondary issue: in segments where all channels failed to meet the threshold, every trace in that range was filtered out. This produced localized blank zones within the seismic line (Figure 10c–d). We kept it blank rather than forcefully including one channel in the entire data to ensure consistency in the quality of processed data (Figure 10d). For intervals where seafloor picking was not feasible, single-channel processed seismic data were used as an alternative for interpretation. Although these data lack the advantages of multi-channel stacking, they still provide valuable insight into subsurface features in otherwise unresolvable sections. In areas of shallow water (<20-30 m), an additional challenge was encountered. Here, the direct arrival and seafloor reflection events occur close in time, making it difficult to apply an effective top mute. This overlap reduced the efficiency of the threshold-based picking approach and limited its applicability in those shallow regions.

Due to time constraints and the generally shallow water depths in the ENS 2022 survey data, swell correction was not applied. Additionally, Channel 9 began at an offset of approximately 15–20 m, which, combined with the shallow conditions, resulted in significant interference between the direct arrival and the seafloor reflection for most channels. The 2022 dataset also exhibited higher noise levels within the water column compared to the 2023 survey. Collectively, these factors made the application of swell correction impractical for the ENS 2022 dataset.

Table 1 Details on data picked using a semi-automated picking approach.

Line	Data / Pick Quality	Mispick Rate	Channel Notes	Additional Remarks
Line01_NS	Generally good quality; shallow depth for first 5000 shots causing higher mispicks on upper channels.	1–2% (Channel 40 up to ~2%)	Channel 40 is included.	Shallow section at start affects accuracy.
Line07_NS	Overall good pick quality, even during swell periods.	<2%	–	Occasional intervals with severe swell cause minor mispicks (1–2%).
Line10_NS	Only the first half of the line (FFID 341300–399300) processed with swell correction.	–	–	Remaining section excluded due to lower quality or depth variation.
Line17_NS	Very high-quality picks with almost no missing values.	<0.05% (≈1 in 2000)	–	Excellent consistency across all channels.
Line33_NS	High data and pick quality.	~0.1% (≈1 in 1000)	Channel 40 is included.	Very few missing picks observed.
Line34_NS	Very high-quality picks overall; performance slightly decreases toward the end.	0.5–1%	–	Degradation linked to increased swell in final section.
Line45_NS	Shallow first half with increased missing picks and mispicks.	1–2%	Only Channels 9–18 usable with NMO; without NMO, more channels can be used.	Interval FFID 2,733,000–2,746,000 too close to direct arrival — poor FBpicks.
Line46_NS	Automated picking limited due to shallow depths and interference between seafloor and direct arrivals.	–	–	Only first part (until FFID 2,872,800) picked with semi-automated routine.
Line47_NS	Shallow line with many missing picks but few mispicks.	<1%	Issues in Channels 34-40 due to direct arrivals.	First ~1000 FFID unpickable; deeper parts picked well.
Line47a_NS	Good performance and stable top mute in shallow parts.	<1% (up to 1% on weaker channels)	Channel 40 included (<2% mispicks).	Generally excellent consistency across line.
Line48_NS	Excellent overall quality with negligible mispicks or missing picks.	~0%	Channel 40 included.	High confidence in automated picks.

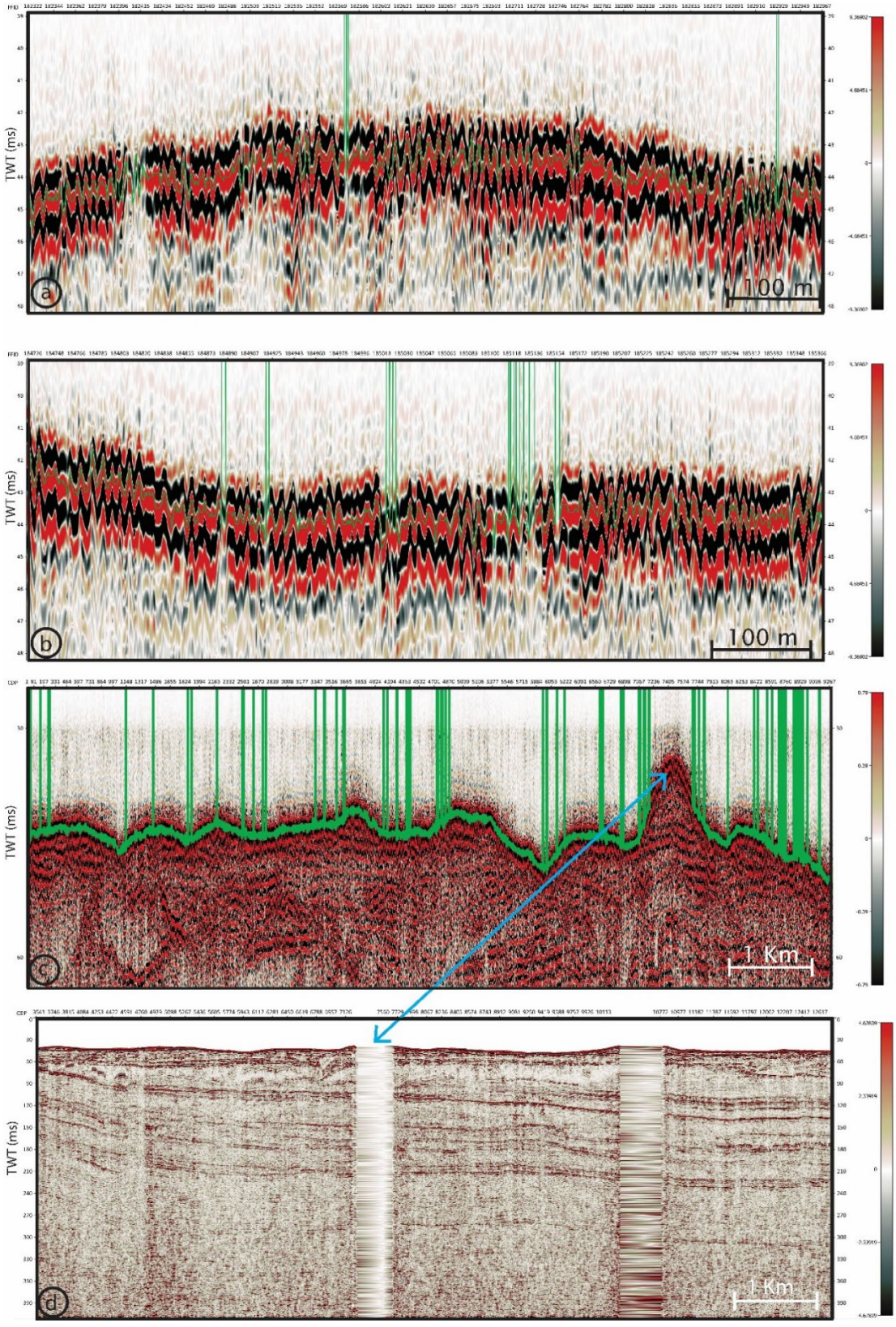

Figure 10 On Line07_NS relatively moderate (a) and bad (b) quality of the picked seafloor from automatic seafloor reflection picking routine. Effect of missing seafloor picks (c) on the processed seismic data (d).

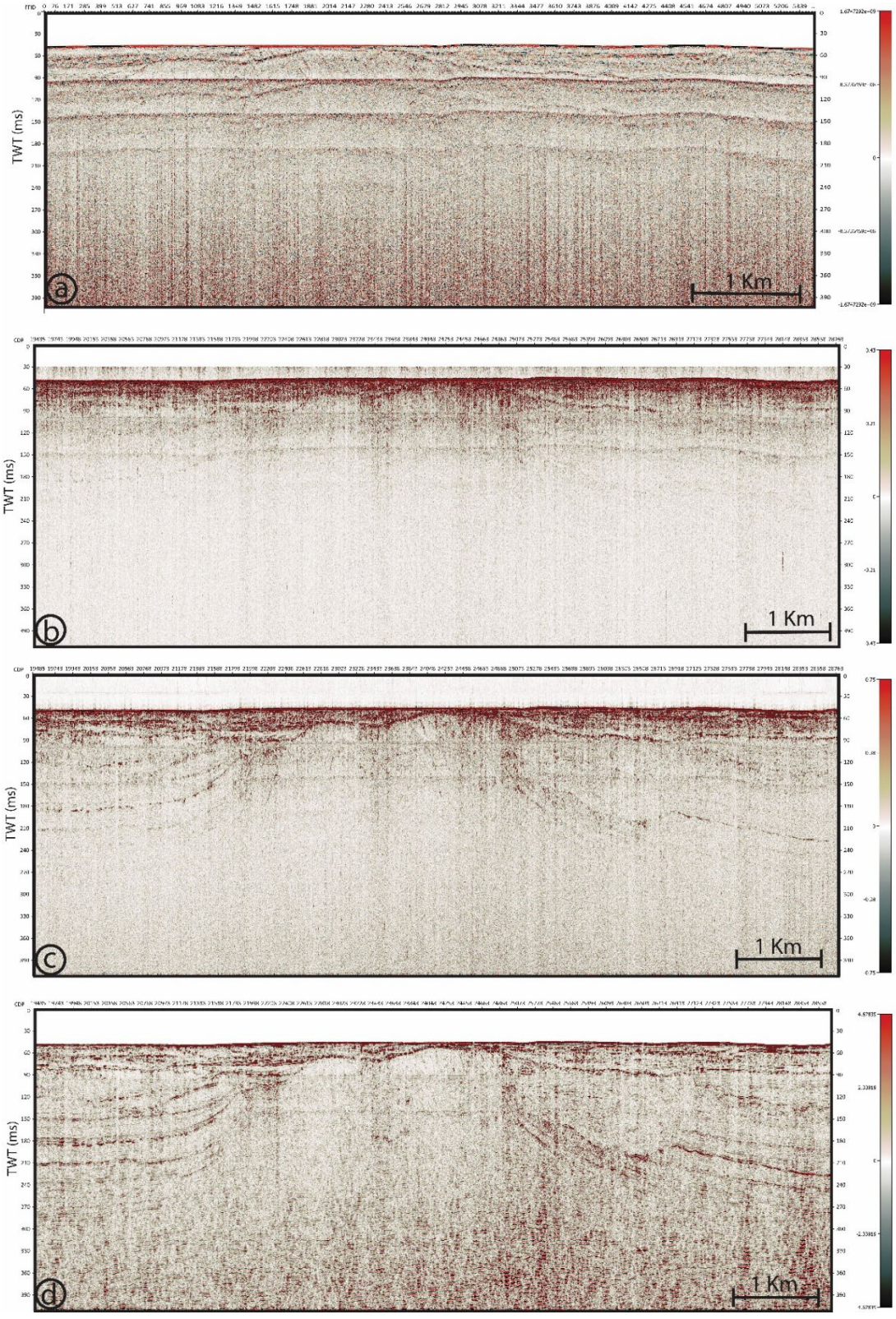

Figure 11 Part of Line07_NS at several stages of processing. (a) Processed single-channel seismic section from Line07_NS, acquired using a single-channel streamer. (b) Stacked seismic section without swell correction. (c) Stacked seismic section after swell correction, using an automatic seafloor picking routine. (d) Final processed seismic dataset.

7. Deghosting and deconvolution

Deghosting was applied to suppress ghost reflections originating from both the source and receiver, using source and receiver depths of approximately 0.4 m. This process enhances wavelet fidelity and improves the overall frequency content of the seismic data. Subsequently, spiking deconvolution was performed to increase vertical resolution by compressing the seismic wavelet and attenuating short-period reverberations.

Initially, both deghosting and deconvolution were applied in the post-stack domain due to limited computational resources. However, following upgrades to the processing infrastructure, these steps were re-implemented in the pre-stack domain for most of the processed lines, enabling more accurate resolution enhancement and improved control over signal characteristics. After the upgrade, most (80–90%) of the data was reprocessed using the pre-stack workflow. For the remaining data, the application of these steps in the pre-stack domain altered the character of the seismic signal in a way that it reduced the ability of removing seismic multiples which partly rely on similarity in the seismic signal. The choice of whether to apply these processes before or after stacking depended on several factors:

- Efficiency of multiple removal in the post-stack domain and its influence on signal quality,
- Water depth, which affects ghost delay and interference patterns,
- Penetration depth and the availability of coherent signal below the first multiple, and
- Computational requirements associated with pre-stack processing.

The combined application of deghosting and deconvolution enhanced the sharpness of the primary reflections, however, also introduced some level of noise (Figure 12; Figure 13; Figure 17b-c).

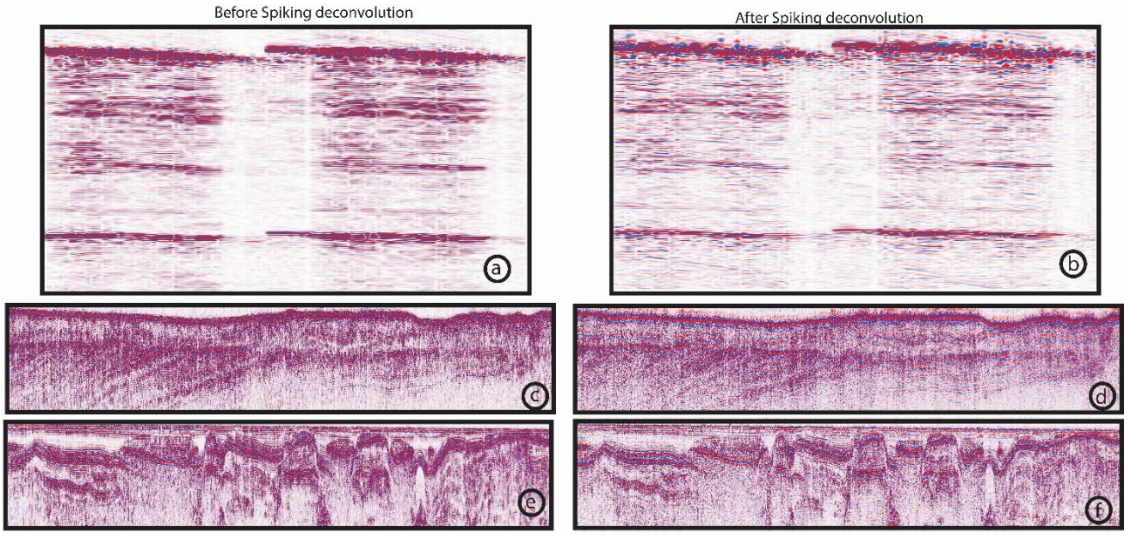

Figure 12 Two shot gathers before (a) and after (b) spiking deconvolution. Seismic sections from Line01_BO after stacking without spiking deconvolution (c and e) and with spiking deconvolution (d and f).

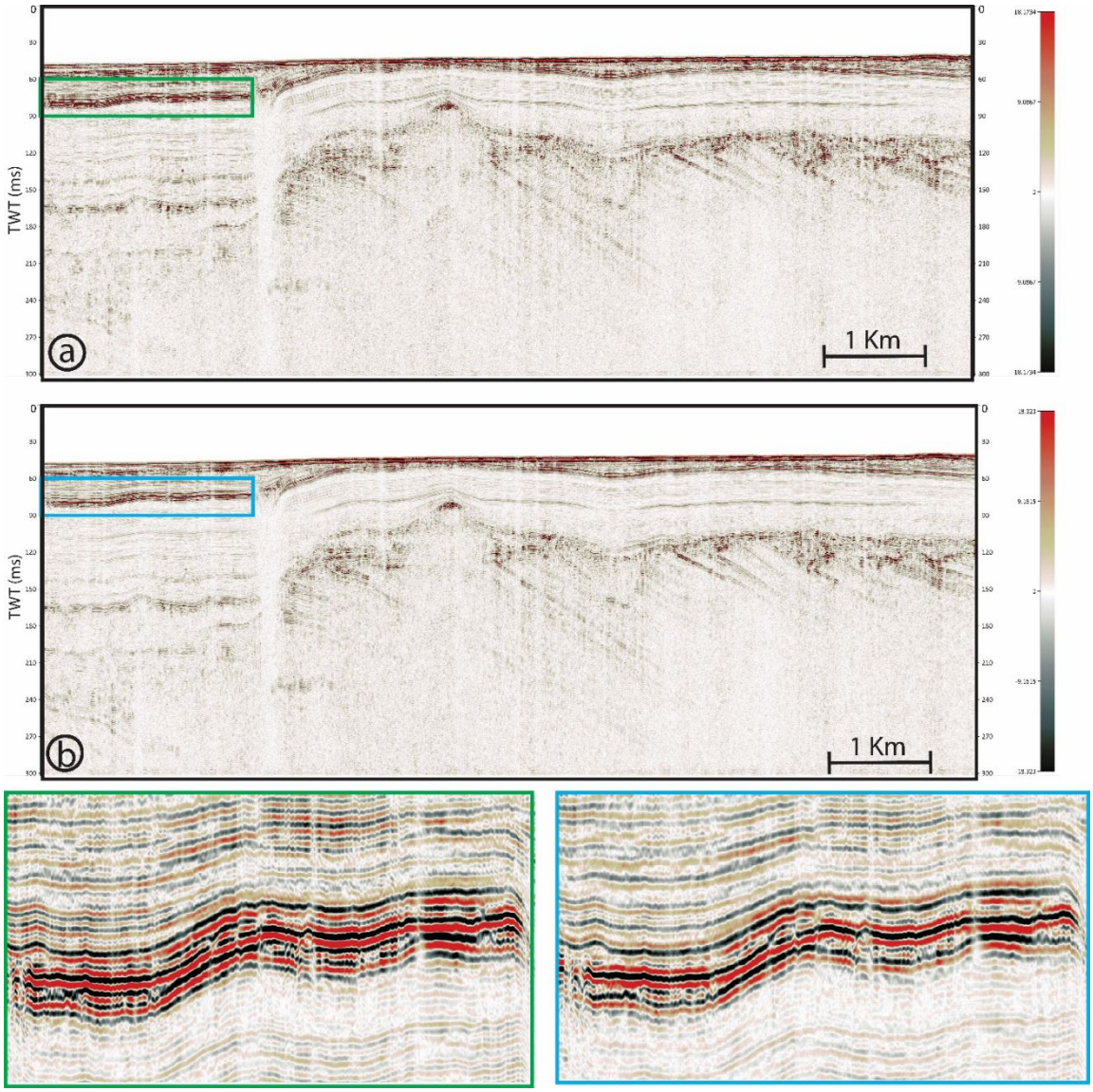

Figure 13 Seismic sections from Line19_AS without (a) and with (b) deghosting and spiking deconvolution.

8. Removal of seismic multiples

The water depth was generally shallower than the penetration depth of the UHRS data into the sediments across most of the survey area, hence, making the removal of seismic multiples essential to reveal geological features masked by strong multiple energy (Figure 11; Figure 14; Figure 15). The strength of water-bottom multiples varied significantly throughout the survey, primarily depending on the reflection coefficient of the seafloor reflection. In many areas within the inner Danish waters, where water depths were particularly shallow, strong water-bottom multiples severely obscured deeper reflectors (Figure 20c-d).

A zero-offset demultiple technique was applied iteratively at several processing stages: before filtering, after F–K filtering, following burst noise removal, and during later steps. This multi-stage approach effectively exploited the slight variations in the expression of the repetitive nature of multiple arrivals, progressively enhancing the recovery of deeper reflectivity.

The algorithm uses adaptive subtraction of a multiple model derived from the data itself, either by static shifting or auto-convolution, with parameters adjusted to account for variations in multiple character and arrival times. The method effectively attenuated water-bottom multiples, especially in areas with minimal swell influence; however, swell-related disturbances sometimes reduced the efficiency due to differences between primaries and multiples. Depending on conditions, the filter sharpness was adjusted, and in some cases, particularly when using static-shift mode, loss of primary energy near the first multiple was observed, as an unavoidable trade-off (Figure 14; Figure 15c; Figure 16c).

In some areas, to prioritize imaging of deeper subsurface features, an aggressive demultiple strategy was deliberately adopted, even at the expense of suppressing some shallow reflections close to the first multiple (Figure 17a). For most of the data, however,the demultiple filter was kept limited, in the senseof removing a minimum amount of primary energy (Figure 11; Figure 15; Figure 16).

In addition to the demultiple routines, the stacking process itself played a crucial role in multiple attenuation. Multiple energy arrives at lower seismic velocities (close to water velocity) compared to seismic velocities of primary events. Hence, stacking velocities were chosen to be slightly higher than optimum as a targeted adjustment that helped further to suppress residual multiple energy during stacking. This careful velocity selection improved the clarity of deeper reflections by minimizing the interference of shallow multiples.

In summary, the combined application of iterative demultiple processing, optimized stacking velocities, and careful stage-wise refinement substantially enhanced the imaging of deeper subsurface structures. Although this approach involved trade-offs in the fidelity of shallow reflections, it provided a much clearer and more reliable view of the geological features beneath the first multiple. However, there are still peg-leg multiples on a few lines which this process did not effectively remove (Figure 17d).

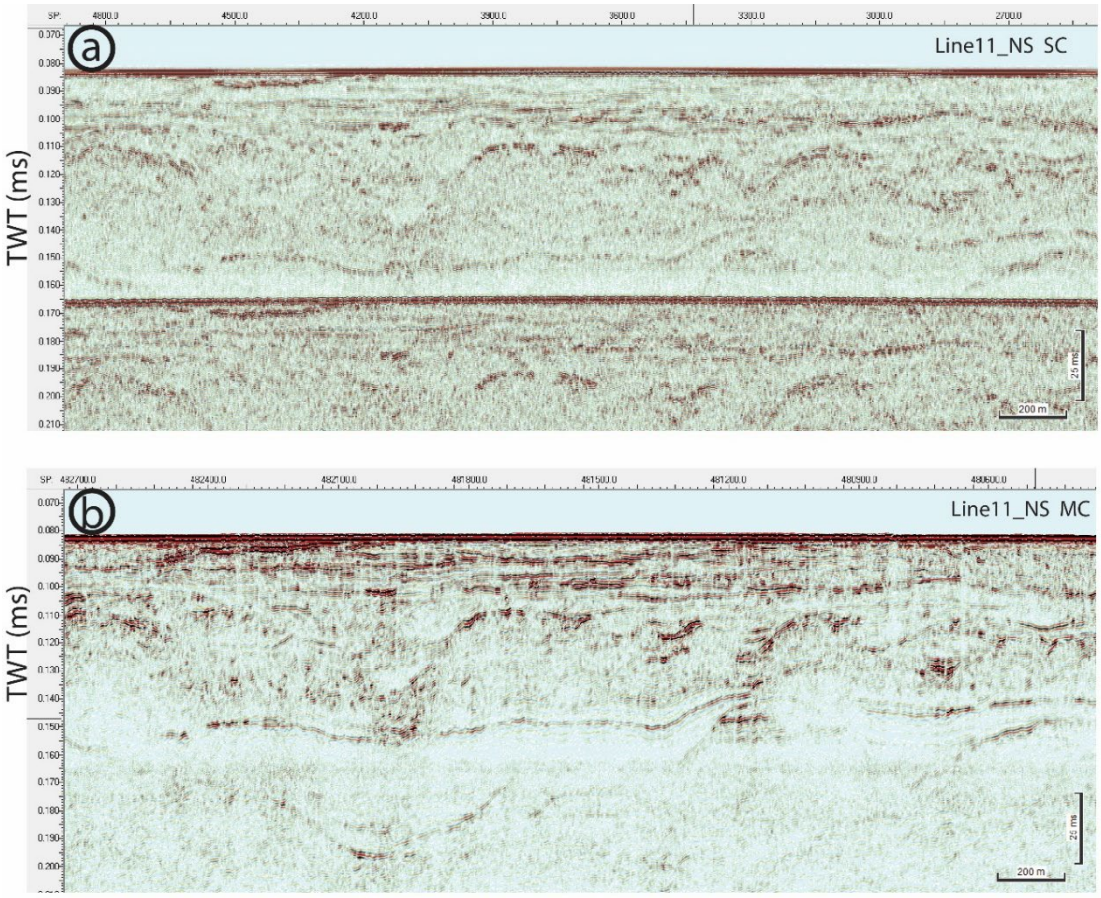

Figure 14 Comparison of processed single-channel (a) and multi-channel (b) seismic data at greater water depths (Line11_NS). Note the strong multiple in the single-channel data.

9. NMO Correction (Normal Moveout) and stacking

Normal Moveout (NMO) correction realigns reflection events in CDP gathers by compensating for travel-time differences caused by source–receiver offsets. This correction assumes a hyperbolic moveout and is fundamental for accurate stacking and velocity analysis. NMO correction was applied at several stages of processing. For F–K and other noise related filtering approaches which require NMO corrected data, NMO correction was performed using a uniform seismic water velocity of 1480 m/s, which helped better elimination of noise and facilitated more effective multiple removal by repetitive application of zero-offset multiple attenuation processing steps. Inverse NMO was applied to bring data back to arrival times.

Prior to stacking, NMO correction was applied again using an interval velocity model. In this model, the water layer velocity was fixed around 1480 m/s, while a uniform seismic velocity was assigned to marine sediments extending approximately 200 ms below the seafloor. The final stacking velocities were determined by inspecting NMO corrections within CDP supergathers, ensuring optimal alignment of reflection events across offsets. Although this approach provided a reasonable balance between accuracy and efficiency, some signal degradation was inevitable. Achieving perfect reflector flattening before stacking would require a high-resolution velocity model capable of capturing small-scale lateral velocity variations, something not feasible with the simplified interval model used here.

To mitigate NMO stretch effects, particularly at far offsets and shallow depths, a stretch mute was applied. This procedure suppressed undesirable stretching artifacts and prevented an increase in noise components, thereby preserving the integrity of the reflection wavelets. Following NMO correction, traces within each CDP gather were stacked to produce a composite trace with enhanced signal-to-noise ratio (SNR). The stacking process reinforced coherent primary reflections while suppressing random and incoherent noise, significantly improving the clarity of the final seismic image and facilitating more reliable geological interpretation.

10. Post-stack processing

10.1 Migration

Migration corrects the seismic image for the effects of dipping reflectors and lateral velocity variations. In the migration process events are repositioned to their correct spatial location in the subsurface, collapsing diffractions and improving structural accuracy and we have used Kirchhoff time migration to migrate the dataset. Slightly lower seismic velocities compared to the seismic velocities used for NMO correction were used for migrating the dataset as stacking velocities were slightly on the higher side. Migration aperture was increased from around 10 m for 30 ms arrival times to 36 m for 400 ms arrival times. In a few (<5%) lines, we do see an artifact in terms of migration smiles or a faint strengthening of reflection parallel to the seafloor (around 10-15 m below the seafloor), after migration of data (Figure 17a).

10.2 Amplitude Corrections and SEG-Y data export

To enhance reflections from the deep subsurface, additional amplitude corrections were applied to compensate for factors that affect seismic signal strength, including geometrical spreading and absorption (Q compensation). A relatively aggressive bandpass filter (100–200–1500–2000 Hz) was also applied before exporting the final data in SEG-Y format. The SEG-Y data was exported with trace sequence number (TRACENO), Line number (R_LINE), CDP number (CDP) and the location of CDP (CDP_X and CDP_Y) locations: TRACENO,4I,,17/ R_LINE,4I,,5/ CDP,4I,,21/ CDP_X,4I,,73/ CDP_Y,4I,, 77.

11. Quality assessment of processed UHRS data

11.1 ENS 2023 survey, North Sea

The quality of the processed seismic data varied notably from line to line (Figure 15). This variation was primarily influenced by the quality of the acquired data which was strongly affected by weather conditions, as well as by the processing workflow, particularly the effectiveness of swell correction (Figure 15b). In addition to these factors, regional geological conditions also played a significant role in controlling the penetration and overall clarity of the seismic signal.

In the North Sea survey (Figure 3), several lines exhibited good seismic penetration, including Lines 01 and 02 (up to 250–300 ms below the seafloor), Line 06 (up to 200 ms), Line 09 (up to 300 ms in parts), Line10, Line17, Lines 29 and 30 (up to 300 ms in some sections), and Line 33 with very good overall penetration. In contrast, Lines 22, 35–38, 43, and 46a–46b (part of lines with shallow water depths) showed limited or poor penetration. The swell-corrected lines with CDP discontinuities causing gaps in the processed MC data include Line 06 and Line 07 (CDP not continuous), Line 10 (CDP not continuous), Line 39 (large CDP jumps at the beginning up to CDP 9378), Line 42 (multiple CDP jumps toward the end), and Line 43 (a swell-picking related CDP jump from CDP 127289 to 127784). For almost all lines, the multi-channel data quality is better than the single-channel data quality. However, on a few lines (Lines 19-21 and 44-46), the quality is comparable in parts of these lines (single-channel data quality is really good with relatively high resolution, Figure 18-d). Lines 47 and 48 have very high uncertainty in CDP locations due to missing navigation data for these lines.

11.2 ENS 2022 survey, Inner Danish Waters

The quality of the processed multi-channel seismic data from the 2022 survey (Figure 2) showed even greater variation compared to the 2023 survey, including the potential variability due to geological factors (Figure 16). Among the surveyed regions, the Anholt South (AS) and Bornholm (BO) areas performed relatively better than the Køge-Krieger (KK), Læsø South (LS), and Vejsnæs Flak (VF) areas. The distance between the source and the streamer had a significant impact on the data quality. In areas where this distance was large and the water depth was shallow, multiples often exhibited higher amplitude than primary reflections, making it impossible to fully suppress them (Figure 20c-d). In such cases, the multiples carried more information about the subsurface than the primary signal itself (Figure 20c-d). This occurred because multiples have a near vertical incidence, whereas primary signals were strongly affected by seafloor reflections and possibly AVO effects, which reduced the transmitted energy at high incidence angles. These issues were most pronounced in the KK, LS, and VF areas, where the quality of the single-channel seismic data was comparable to the

quality of the multi-channel data because the single-channel streamer was placed closer to source, thereby creating near vertical incidences. Due to these reasons, single-channel seismic data from KK, LS and VF areas were reprocessed in RadexPro to get the best possible result. In contrast, data acquisition in the Læsø North (LN) area was largely unsuccessful - likely due to poor weather conditions and possible sparker system malfunction. The resulting data contained very little usable signal, leading to the abandonment of further processing for this area due to extremely poor data quality.

LS area
In this area the seismic data generally shows poor penetration and shallow water depths. Lines 11 and 17–18 exhibit significant CDP jumps.

AS area
Here lines with good to very good penetration includes Lines 15, 18, 19, 20, 21_T, and 22–24, while Lines 16 and 17 shows normal penetration. Conversely, several lines exhibit limited or poor penetration, including Lines 02, 04, 08–14, 10, and 11, with Lines 12 and 13 being particularly poor. Some lines, such as 07, show variable penetration and quality but were generally better than single-channel data.

VF area
In this area water depths were also very shallow and penetration is limited up to 30-50 ms below the seafloor for most seismic lines.

KK area
In the KK area, penetration was generally poor, probably due to shallow water depths and/or geological conditions in terms of a hard seabed. Lines 01–03 had shallow water depths with seafloor arrivals around 20–30 ms. While Lines 01–04 reached only 40 ms of penetration, line 07 showed 20–50 ms penetration, with better image quality at deeper offsets. Lines 13–15 shows almost zero penetration. In some parts of this area, multiples appear to be of greater strength compared to the primary signal (Figure 20c-d).

BO area
In the BO area, penetration varies widely due to geological variability and differences in frequency filtering. Lines 01–03 and 11 shows highly variable penetration from very good to very poor, likely due to subsurface heterogeneity. Line 12 has very deep penetration with effective multiple removal. Lines 13–15 showa limited penetration due to hard seafloor. Line 16 exhibit variable penetration and only moderate multiple removal quality, with many dipping reflectors. Lines 17–18 shows good penetration and multiple removal, while Line 19 is chaotic due to lateral velocity variations affecting stacking. Higher frequency filtering in BO lines appeared to reduce noise, possibly unmasking effects from shallow gas.

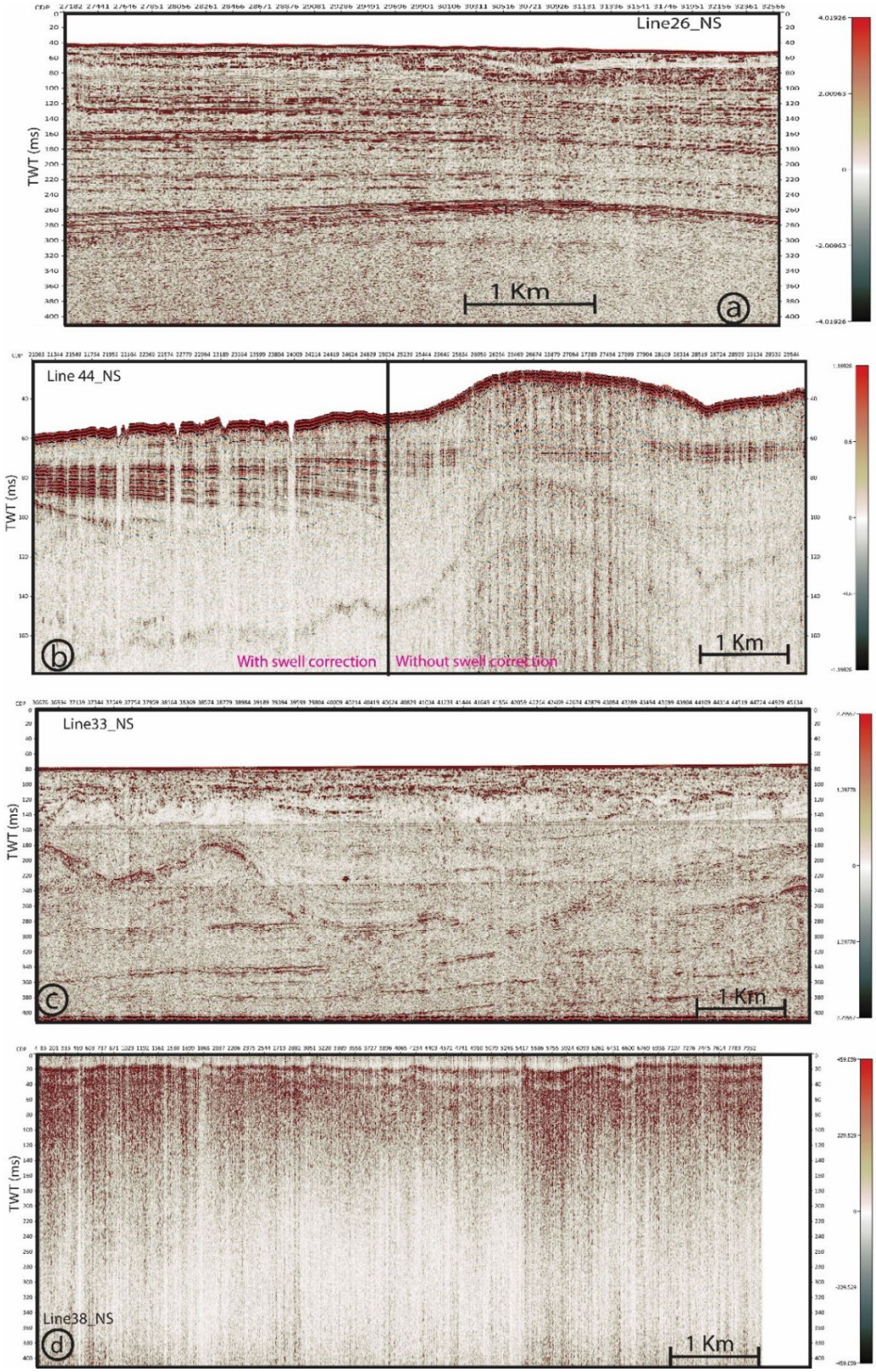

Figure 15 Variability in the processed dataset from the ENS 2023 survey with good (a and c) to bad (b) penetration of seismic signal and poor data quality due to bad weather (d). Difference in the quality with and without swell correction (b) for the same line.

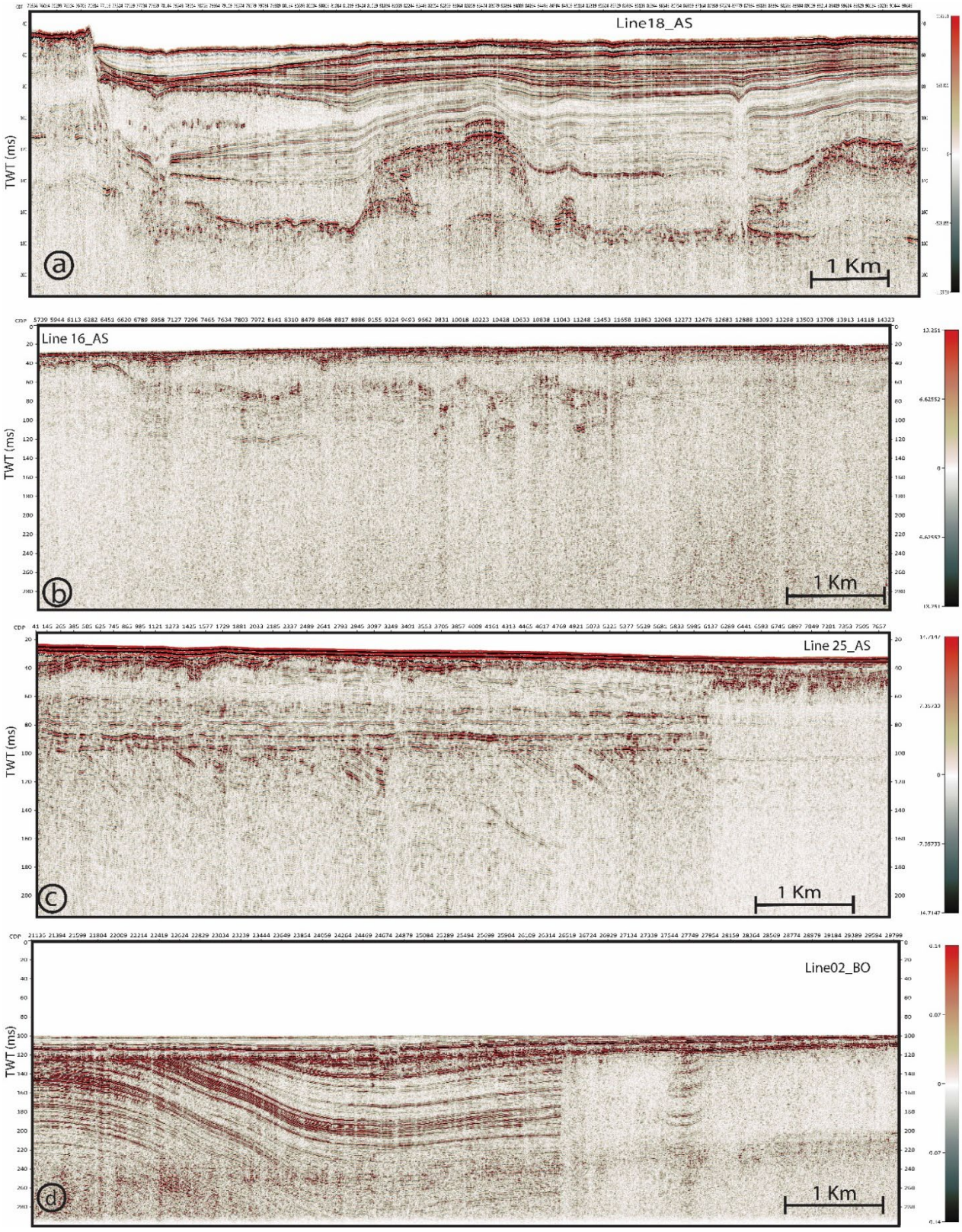

Figure 16 Variability in the processed dataset from the ENS 2022 survey with good (a and d) to bad (b) penetration of seismic signal. Difference in the penetration due to geological factors (c and d).

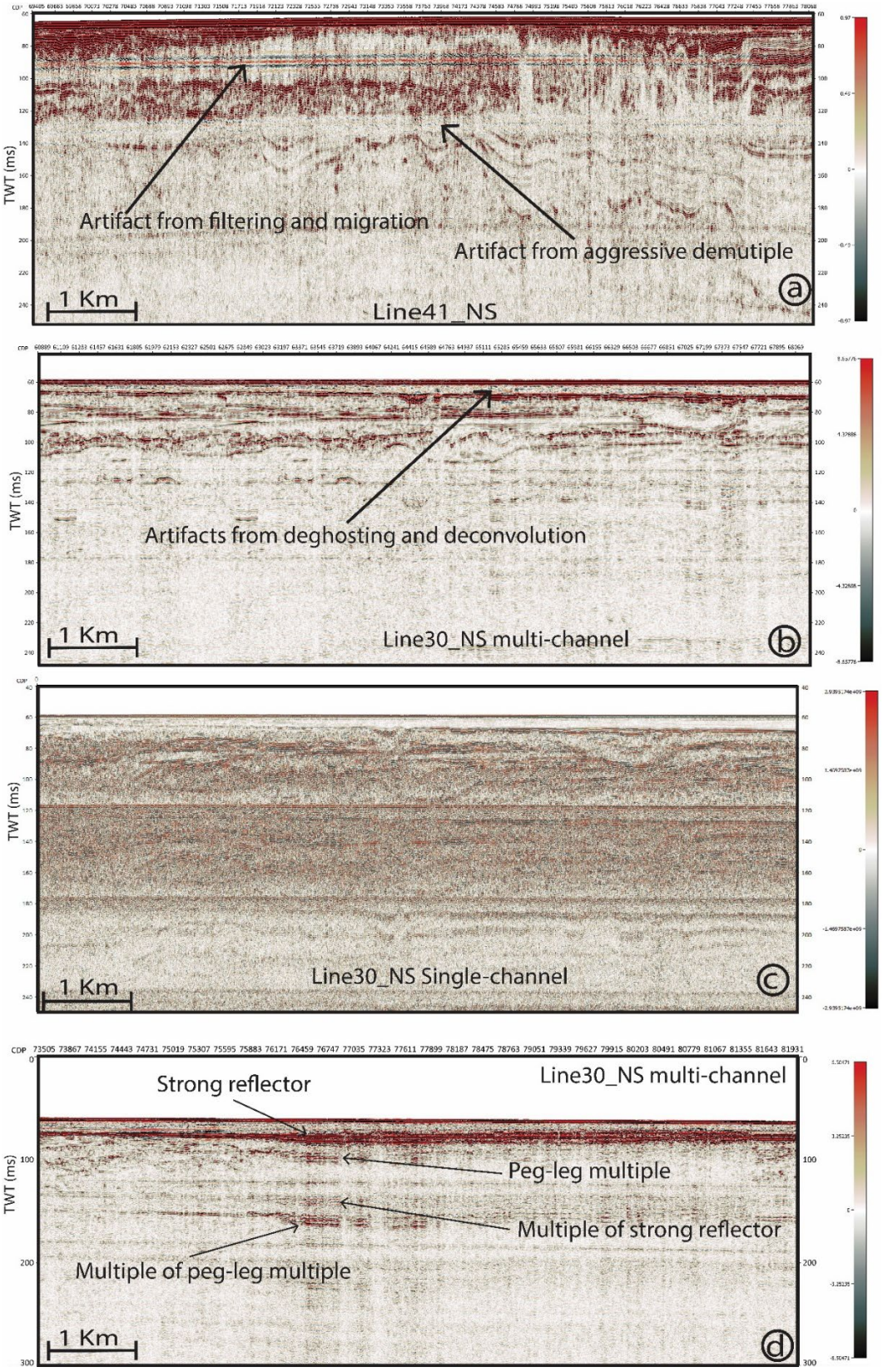

Figure 17 Processing artifacts due to filtering and migration (a), deconvolution and deghosting (b and c) and peg-leg multiples (d).

12. Evaluation of the processed seismic data

The difference in data quality between single-channel (SC) and multi-channel (MC) streamer systems primarily arose from two factors:

1. Streamer offset: The single-channel streamer was positioned much closer to the source. This was particularly significant in the ENS 2022 survey, where the useful channels of the multi-channel streamer were located at offsets of 15–20 m. The effect of this offset was especially pronounced in shallow-water environments (Figure 20).
2. Streamer depth: The single-channel streamer was deployed closer to the sea surface, producing a more spiky (sharp) signal. While this degraded imaging capability at greater depths, it enhanced resolution in very shallow sections immediately below the seafloor, where SC data often produced superior results (Figure 18).
3. Illumination differences: Since the SC and MC systems were located on two opposite sides from the source, the difference in raypaths can create differences in the illumination of horizons (Figure 19a-b).

Interestingly, certain geological features absent in one dataset (SC or MC) appeared clearly in the other. This is likely due to differences in raypath geometry and horizon illumination at varying incidence angles (CDP range 9500–11 000 in Figure 19a–b). Furthermore, variations in frequency content and filtering may have reduced noise in one dataset, revealing potential masking effects caused by gas (Figure 19c–d). A combined interpretation of both SC and MC datasets therefore provides a more reliable understanding and helps minimize interpretational errors.

In general, for water depths greater than ~30 m, multi-channel seismic data performed significantly better, even with the larger source-streamer offset. However, a sharp drop in processed data quality was observed as water depth transitioned from deep to shallow zones (Figure 20), particularly in the ENS 2022 survey where the offset between the source and the first high-quality channel exceeded 15 m.

For the Læsø South (LS), Vejsnæs Flak (VF), and Køge-Krieger (KK) areas of the ENS 2022 survey (Figure 2), the single-channel streamer data exhibited significantly better quality than individual channels from the multi-channel streamer. This difference was mainly due to the shorter source–receiver offset of the SC system. Consequently, SC data from these areas were optimally processed using additional filtering, migration, and demultiple steps to extract geological information.

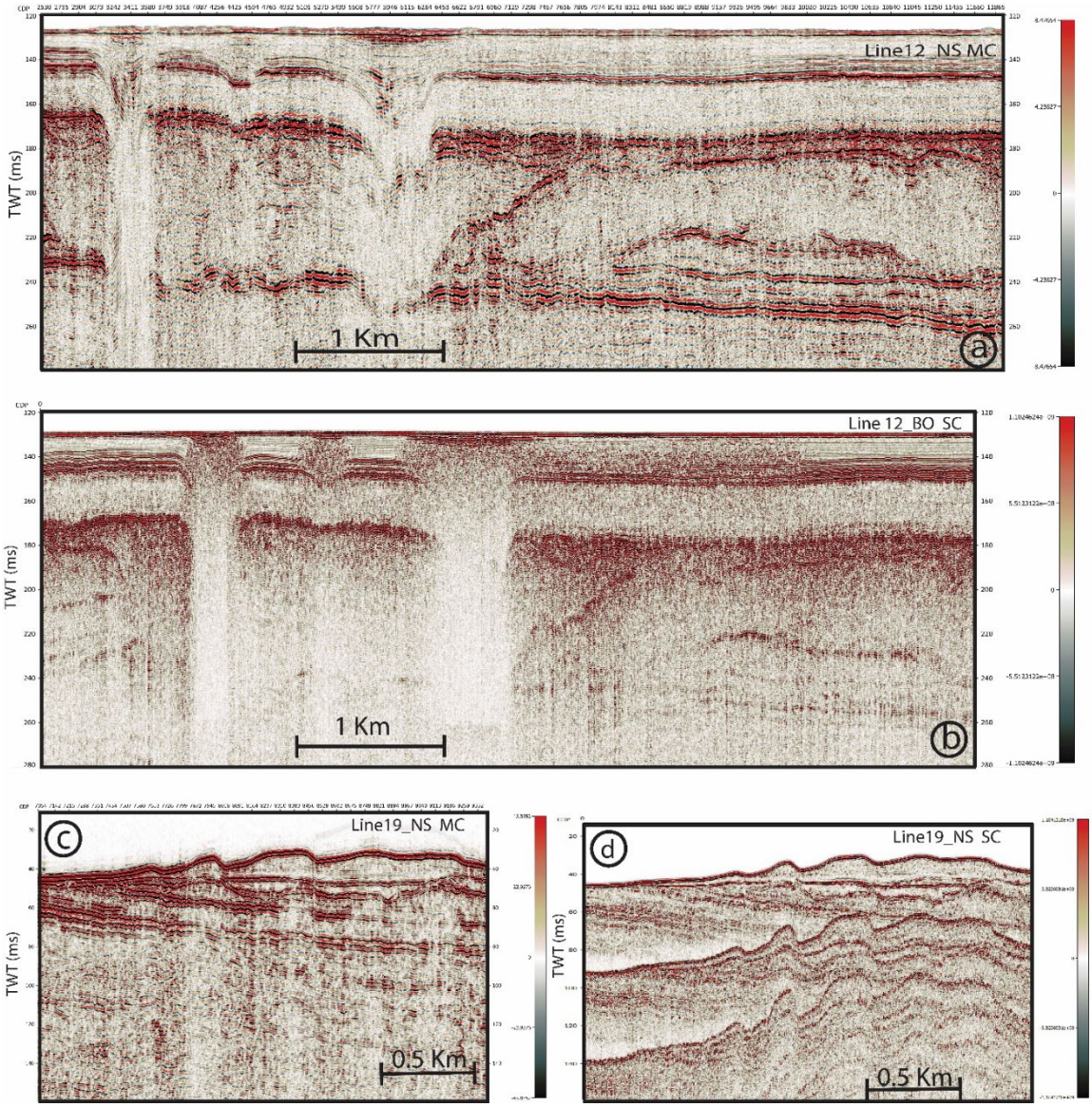

Figure 18 Difference in the processed seismic data from SC and MC and effect of water depth and depth below the seafloor on the imaging quality from SC and MC.

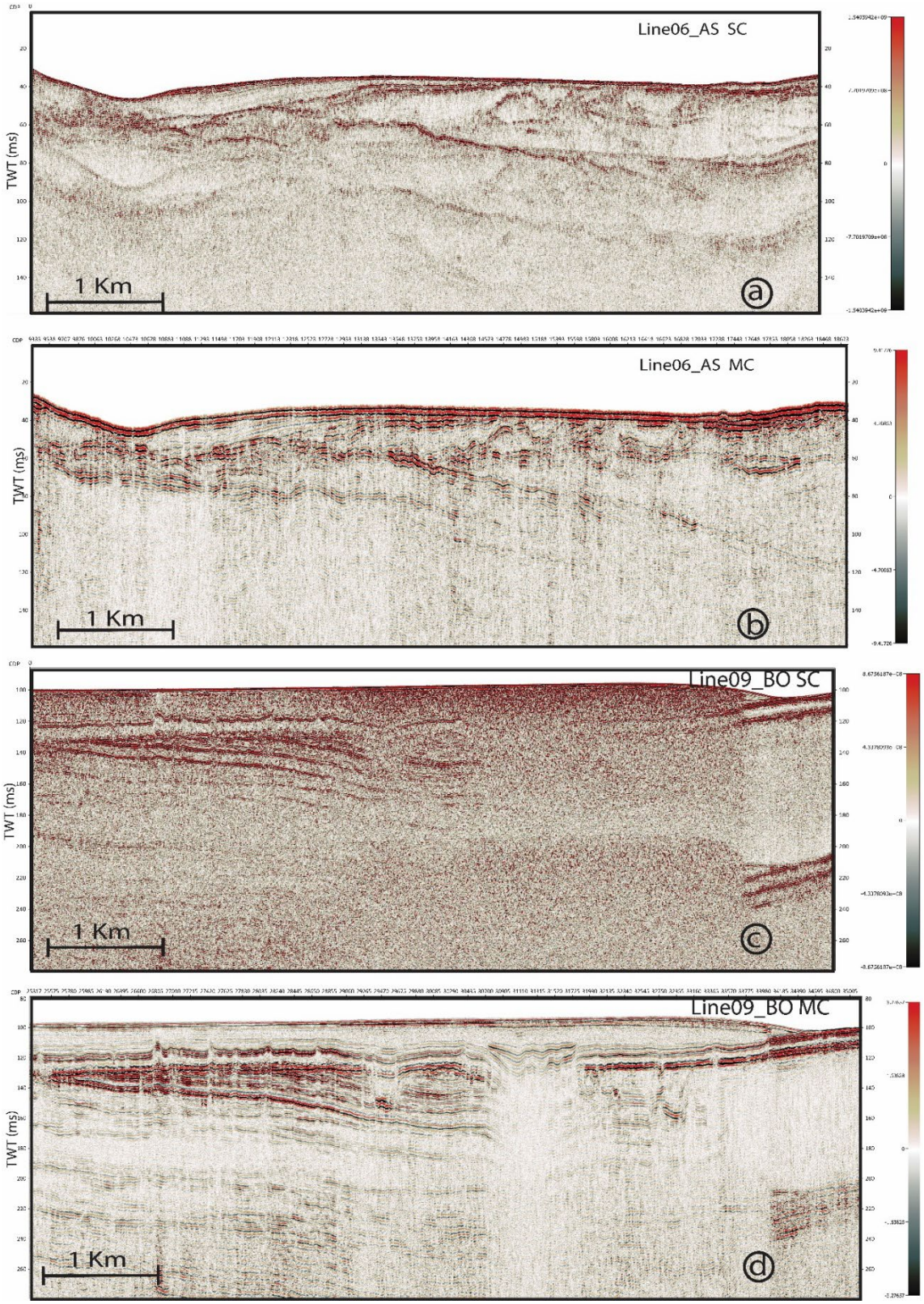

Figure 19 Highlighting the potential utility of combined interpretation from processed MC and SC data as they may highlight different features. Single-channel and multi-channel seismic section from lines (Line06_AS and Line09_BO).

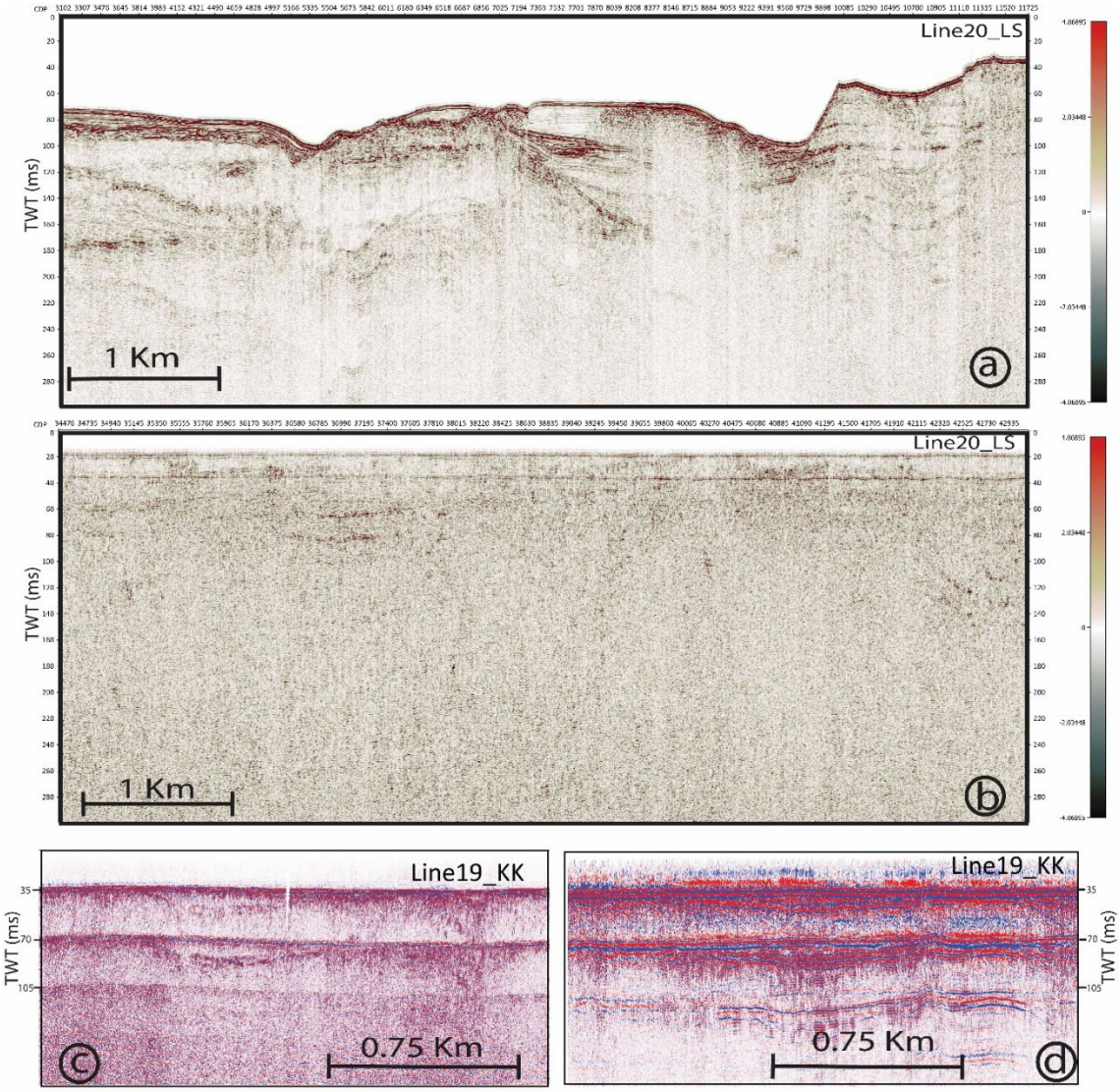

Figure 20 Effect of water depth of the quality of subsurface imaging from multi-channel seismic in ENS 2022 survey.

13. Artifacts and noise induced by the processing

Artifacts in the processed seismic data primarily originated from filtering, demultiple processes, migration, deconvolution, and deghosting steps. The combined effect of bandpass filtering applied after top muting, followed by migration, produced artificial reflections parallel to the seafloor in several processed seismic lines (Figure 17a). This artifact is particularly prominent on lines 39–43_NS) of the ENS 2023 survey (Figure 3). Migration "smiles," often occurring in zones likely associated with gas presence, were observed on only a few processed lines.

Both deconvolution and deghosting introduced additional noise as the signal became more spiky (sharp) (Figure 17b). The same areas, when examined in single-channel seismic data, appear relatively blank (Figure 17c). Such chaotic signals can misleadingly suggest complex subsurface geology in areas that are otherwise stratigraphically uniform.

The application of the demultiple approach likely introduced the strongest artifacts in the processed data (Figure 17a). While more aggressive multiple removal enhanced imaging at greater depths, it also resulted in the loss of primary signal near the first seabed multiple. Processing parameters were therefore carefully adjusted to balance between deeper visibility and signal preservation. The variable extent of this "blanking" effect can be seen near expected seabed multiples (Figure 11; Figure 14; Figure 17; Figure 18; Figure 19). In some cases, interpretations can be aided by using single-channel data to trace reflector continuity where signals are wiped out by demultiple processing.

In several lines, high-amplitude reflections appear toward the end of the seismic record (Figure 15c). These are likely processing artifacts that could have been mitigated by bottom muting the last 5–6 ms of data. Since this correction was not applied, care must be taken to avoid interpreting these flat, high-amplitude features as genuine horizons.

Finally, potential peg-leg multiples remain visible in some processed sections (Figure 17d). These are particularly misleading because most primary multiples have been removed, making peg-legs appear as genuine geological reflectors. Interpreters should exercise caution and critically evaluate such features during the geological interpretation.

14. References

Pérez, L. F., Hansen, L. Ø., Vangkilde-Pedersen, T., Christensen, N., Andersen, M. S., Allaart, L., Rödel, L.-G., Andersen, S. B., Haase, E. J., Baltz, A. K., Przyswitt, Z., & Nielsen, C. E. (2023). Survey report for the inner Danish waters and the Baltic Sea around Bornholm, 2022. Geological screening for offshore wind farms, the Danish Energy Agency. GEUS. Danmarks og Grønlands Geologiske Undersøgelse Rapport Vol. 2023 No. 10. https://doi.org/10.22008/gpub/34677

Vangkilde-Pedersen, T., Pérez, L. F., Nørgaard-Pedersen, N., Winther, L. H., Rödel, L.-G., Andersen, S. B., Christensen, N., Allaart, L., Stenshøj, R. Ø., Pedersen, L. L., Everding, L., & Andersen, R. (2023). Survey report for the Danish North Sea, 2023: Geological screening for offshore wind farms, the Danish Energy Agency. GEUS. Danmarks og Grønlands Geologiske Undersøgelse Rapport Vol. 2023 No. 25. https://doi.org/10.22008/gpub/34692

Vangkilde-Pedersen, T. G., Christensen, N., Nørgaard-Pedersen, N., Allaart, L., Bennike, O., Leth, J. O., Winther, L. H., Sandersen, P., Prins, L. T., Singhroha, S., & Pérez, L. F. (2025). Bedre geologiske data til udbygning af havvind - Overordnet geologisk kortlægning af det danske havområde for Energistyrelsen. GEUS. Danmarks og Grønlands Geologiske Undersøgelse Rapport Vol. 2025 No. 29. https://doi.org/10.22008/gpub/34786

Danish Ministry of Climate,
Energy and Utilities

Geological survey of
Denmark and Greenland (GEUS)

Øster Voldgade 10
DK-1350 Copenhagen K
Denmark

GEUS is a research and advisory institution in the Danish Ministry of Climate, Energy and Utilities